Uncertainties in theoretical predictions for $\gamma d \to \pi^0 d$ observables near threshold due to the use of different elementary amplitudes

H. M. Al-Ghamdi[a], E. M. Darwish[b,c,*], A. A. Ibraheem[d,e] and H. M. Abou-Elsebaa[b,c]

[a]*Physics Department, College of Science, Princess Nourah bint, Abdulrahman University, P. O. Box 84428, Riyadh 11671, Saudi Arabia.*
[b]*Physics Department, Faculty of Science, Taibah University, Medina 41411, Saudi Arabia.*
e-mail: darwish@science.sohag.edu.eg.
[c]*Physics Department, Faculty of Science, Sohag University, Sohag 82524, Egypt.*
[d]*Physics Department, Faculty of Science, King Khalid University, Abha 62529, Saudi Arabia.*
[e]*Physics Department, Faculty of Science, Al-Azhar University, Assiut Branch, Assiut 71524, Egypt.*

Received 16 March 2022; accepted 31 March 2022

We discuss possible uncertainties in theoretical predictions for $\gamma d \to \pi^0 d$ observables near threshold due to the use of different elementary $\gamma N \to \pi N$ amplitudes using an approach which is based on time-ordered perturbation theory. Results are presented for unpolarized cross sections and all possible spin asymmetries of differential and total cross sections. Our results indicate that the estimations of the uncertainty on the $\gamma d \to \pi^0 d$ observables show important sensitivity to the modeling of the elementary $\gamma N \to \pi N$ operator. A comparison to presently available experimental data is given. The results presented here are of particular interest for the evaluation of the systematic uncertainties caused by the use of different elementary operators in the analyses of $\gamma d \to \pi^0 d$ measurements to extract information on the free neutron amplitude from deuteron data.

Keywords: Meson production; photoproduction reactions; few-body systems, deuteron; polarization phenomena in reactions; spin observables; polarized beams; polarized targets.

DOI: https://doi.org/10.31349/RevMexFis.68.061201

1. Introduction

Understanding the internal structure and reactions of nuclear systems from first principles was, for a long time, an important goal of nuclear and particle physics. In this regard, few- and many-body systems provide a unique laboratory for studying nuclear interactions. Recent years have witnessed interesting developments in coherent and incoherent pion photoproduction on the deuteron and light nuclei, since relevant experimental studies have been performed (see Refs. [1–14] and references therein). These reactions can be utilized to investigate the internal structure of hadrons in the non-perturbative domain of Quantum Chromodynamics (QCD) and study the behavior of nucleon resonances in the nuclear medium.

In particular, the reaction $\gamma d \to \pi^0 d$ may be used as an isospin filter and it is sensitive to the coherent sum of the proton and neutron amplitudes $\gamma p \to \pi^0 p$ and $\gamma n \to \pi^0 n$, respectively. The $\gamma d \to \pi^0 d$ reaction near π-threshold serves also as a test of our understanding of the chiral πN dynamics. The use of deuteron as an effective neutron target allows one to gain abundant information on the mechanisms of the elementary pion photoproduction off free neutron which otherwise is not possible due to the absence of any stable, dense, free-neutron targets. Furthermore, the deuteron represents also an ideal object for the study of NN interactions.

So far, many studies have been carried out dealing with the reaction $\gamma d \to \pi^0 d$ in the photon energy region from π-threshold up to 1 GeV in order to obtain information on π^0-photoproduction off free neutrons [15–33]. In spite of all these great theoretical efforts, a good description of the experimental data has not been yet found [3, 4, 6, 7]. The disagreement between theoretical models and experimental data may be indicative of shortcomings in the elementary $\gamma N \to \pi N$ amplitudes. It was found in Refs. [34–39] that the $\gamma d \to \pi NN$ observables near π-threshold are considerably dependent on the elementary $\gamma N \to \pi N$ amplitude. During the last decades, more realistic models for the $\gamma N \to \pi N$ amplitude have been constructed [40–48]. Therefore, the construction of more realistic models for the investigation of the electromagnetic pion photo- and electroproduction processes on the deuteron and light nuclei remain challenging.

In addition, theoretical models which consider polarization observables for the reaction $\gamma d \to \pi^0 d$ near π-threshold are very rare. Indeed, polarization observables constitute much more stringent tests of theoretical models. For instance, the helicity dependent total cross sections with respect to parallel (σ^P) and antiparallel (σ^A) spins of photon and deuteron provide important information on the nucleon spin structure. These cross sections are also required to test the validity of the Gerasimov-Drell-Hearn (GDH) sum rule [49]. Furthermore, the deuteron spin asymmetry $\sigma^P - \sigma^A$ and the helicity E-asymmetry contain very interesting physics with respect to the internal hadron structure. Moreover, the double spin asymmetry T^c_{10} for circular polarized photons and vector polarized deuterons is also of great interest. It gives additional

important information on the internal spin structure of the deuteron and provides a direct extraction of the GDH sum rule [49].

Therefore, the main aim of the present work is to discuss theoretical uncertainties in the analyses of $\gamma d \to \pi^0 d$ observables near π-threshold due to the use of elementary $\gamma N \to \pi N$ amplitudes. Since the extraction of the elementary $\gamma p \to \pi^0 p$ and $\gamma n \to \pi^0 n$ amplitudes essentially relies on an interpretation in terms of the plane-wave impulse approximation (PWIA), it is necessary to study its validity, i.e., to have a quantitative estimate of all possible mechanisms going beyond the PWIA. However, in the present paper we want to restrict ourselves to the PWIA while a more realistic treatment including all possible reaction mechanisms will be reported in a forthcoming paper. Here, we want to explore the impact on the description of the $\gamma d \to \pi^0 d$ observables from the choice of the pion photoproduction amplitudes off protons and neutrons. To the best of our knowledge, this has not been studied previously in the literature. We also investigate whether the uncertainties caused by the use of different elementary operators for the predictions of polarization observables in the $\gamma d \to \pi N N$ reaction channels [34–39] are also seen in the analyses of the coherent π^0-photoproduction off deuterons, $\gamma d \to \pi^0 d$. It was demonstrated in Ref. [1] that the single- and double-polarization observables will allow us to select between different models for pion photoproduction on the nucleon.

Most recently, the sensitivity of the results for single-spin asymmetries and the helicity E-asymmetry in the $\gamma d \to \pi^0 d$ reaction near threshold to the choice of the pion photoproduction amplitude has been investigated [33]. Unfortunately, the results presented in that work are based on an error in the definitions of initial and final relative momenta of the two nucleons in the deuteron process. Because of that the corresponding total energy of the photon-nucleon (γN) subsystem was not properly defined, but it strongly affects the predicted results especially at photon lab-energies close to π-threshold and forward pion angles. Thus, the importance of theoretical uncertainties in the $\gamma d \to \pi^0 d$ observables still requires a more careful treatment as done in Ref. [33].

Therefore, the present work was motivated to present results for the unpolarized differential and total cross sections as well as for all possible beam, target, and beam-target spin asymmetries of the differential and total cross sections in the photon energy region from near π-threshold to 170 MeV. As elementary amplitudes, the one provided by the unitary isobar MAID-2007 model from [46] and those obtained using the Dubna-Mainz-Taipei dynamical model (DMT-2001) [47] and the chiral MAID model (χMAID-2013) [48] are used. Furthermore, we compare our results for the unpolarized differential cross section with the experimental data from TAPS [4]. In this comparison with experiment we concentrate our discussion on the unpolarized differential cross section, because data for polarization observables are still not available. The calculations presented in this paper are of particular interest for the evaluation of the systematic uncertainties caused by the use of different elementary operators in the analyses of $\gamma d \to \pi^0 d$ measurements. These uncertainties should be kept in mind when extracting information on the free neutron amplitude from experimental data on the deuteron.

This paper is structured as follows. In Sec. 2, we briefly outline the theoretical framework used to describe the $\gamma d \to \pi^0 d$ reaction. We give the explicit expressions for the $\gamma d \to \pi^0 d$ observables in terms of the reduced t-matrix elements. Subsequently, we calculate the scattering amplitude for this reaction based on time-ordered perturbation theory. Section 3 is devoted to the main results together with a comparison with the available experimental data. Finally, we summarize our results in Sec. 4.

2. Theoretical framework

In this section we briefly describe the theoretical framework for the coherent π^0-photoproduction reaction on the deuteron. We would like to mention that the general formalism for the $\gamma d \to \pi^0 d$ reaction has been described in Ref. [29], and we refer the reader to that work for further details. Here, we briefly recall the necessary notation and definitions.

2.1. Cross section and observables

We consider the reaction $\gamma d \to \pi^0 d$ in the photon-deuteron (γd) center-of-momentum (c.m.). We use a coordinate system with the z-axis along the photon momentum $\vec{k}$ ($\vec{e}_z = \hat{k} = \vec{k}/k$), the y-axis parallel to $\vec{k} \times \vec{q}$, and the x-axis in the direction of maximal linear photon polarization [50], in which the pion momentum $\vec{q}$ has spherical coordinates θ and ϕ. If the incoming photon beam is not linearly polarized, then the x-axis may be chosen arbitrary, and there is no dependence on the angle ϕ. For the deuteron states, a non-covariant normalization following to the conventions of Ref. [51] is used. The initial and final total three-momenta of the two nucleons in

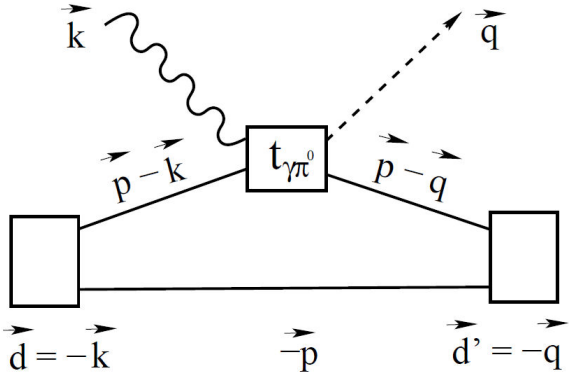

FIGURE 1. Diagrammatic representation of the $\gamma d \to \pi^0 d$ reaction in the impulse approximation with definition of momenta in the γd c.m. system. The spectator nucleon is on-shell.

the deuteron are given in the c.m. system by $\vec{P} = \vec{p}_1 + \vec{p}_2 = -\vec{k}$ and $\vec{P}' = \vec{p}\,'_1 + \vec{p}\,'_2 = -\vec{q}$, respectively. For the initial and final relative three-momenta of the two nucleons in the deuteron in the c.m. system, we obtain $\vec{p}_r = (\vec{p}_1 - \vec{p}_2)/2 = \vec{p} - \vec{k}/2$ and $\vec{p}\,'_r = (\vec{p}\,'_1 - \vec{p}\,'_2)/2 = \vec{p} - \vec{q}/2$, respectively (see Fig. 1).

The cross section for arbitrary polarized photons and initial deuterons can be calculated for a given transition $\mathcal{M}$-matrix by applying the density matrix formalism [50]. All different cross sections for the $\gamma d \to \pi^0 d$ reaction have the form:

$$\mathcal{O} = \mathcal{K} \sum_{\widetilde{m}'_d \widetilde{\lambda} \widetilde{m}_d} \sum_{m'_d \lambda m_d} \mathcal{M}^*_{\widetilde{m}'_d \widetilde{\lambda} \widetilde{m}_d} \Omega_{\widetilde{m}'_d m'_d} \mathcal{M}_{m'_d \lambda m_d} \rho^{\gamma}_{\lambda \widetilde{\lambda}} \rho^{d}_{m_d \widetilde{m}_d} \,, \tag{1}$$

where $\mathcal{K}$ is a kinematic factor, $\mathcal{M}_{m'_d \lambda m_d}$ the scattering matrix, ρ^{γ} (ρ^d) the density matrix for incoming photon (initial deuteron) polarization, m_d (m'_d) the spin projection of the initial (final) deuteron, and $\lambda = \pm 1$ the circular photon polarization. A polarimeter for the deuteron in the final state is described by the operator Ω. In the present work, we set $\Omega = 1$, because we do not consider any polarization analysis of the final deuteron. The scattering $\mathcal{M}_{m'_d \lambda m_d}$-matrix is given by isolating the azimuthal dependence as follows [17, 22]:

$$\mathcal{M}_{m'_d \lambda m_d}(\theta, \phi) = e^{i(\lambda + m_d)\phi}\, t_{m'_d \lambda m_d}(\theta) \,, \tag{2}$$

where the reduced t-matrix elements are defined by separating the ϕ-dependence from the $\mathcal{M}$-matrix elements. Parity conservation gives for the t-matrix the symmetry:

$$t_{-m'_d -\lambda -m_d} = (-1)^{1 + m'_d + \lambda + m_d}\, t_{m'_d \lambda m_d} \,. \tag{3}$$

The kinematic factor $\mathcal{K}$ is given in the γd c.m. frame by:

$$\mathcal{K} = \frac{1}{16\pi^2} \frac{E_d E'_d}{W^2_{\gamma d}} \frac{q}{k} \,, \tag{4}$$

where the deuteron energies in the initial and final states are given by $E_d = \sqrt{M_d^2 + k^2}$ and $E'_d = \sqrt{M_d^2 + q^2}$, respectively, with M_d as deuteron mass. The absolute values of the photon and pion three-momenta in the γd c.m. frame are given, respectively, by:

$$k = \frac{1}{2W_{\gamma d}} (W^2_{\gamma d} - M^2_d) \quad \text{and} \quad q = \frac{1}{2W_{\gamma d}} \sqrt{[W^2_{\gamma d} - (M_d - m_\pi)^2][W^2_{\gamma d} - (M_d + m_\pi)^2]} \,. \tag{5}$$

The invariant energy of the γd system is given as:

$$W_{\gamma d} = E_\gamma + E_d = k + \sqrt{M_d^2 + k^2} \,, = E_\pi + E'_d = \sqrt{m_\pi^2 + q^2} + \sqrt{M_d^2 + q^2} \,, = \sqrt{M_d^2 + 2M_d E_\gamma} \,, \tag{6}$$

where m_π is the neutral-pion mass.

Following the rules of Ref. [52], we write the differential cross section in terms of the unpolarized differential cross section $d\sigma_0/d\Omega$ and the various spin asymmetries Σ, T_{IM}, T^c_{IM}, and T^l_{IM} as follows:

$$\begin{aligned} \frac{d\sigma}{d\Omega} = \frac{d\sigma_0}{d\Omega} \Big[1 + P^\gamma_l \Big\{ \Sigma \cos 2\phi + \sum_{I=1}^{2} P^d_I \sum_{M=-I}^{I} T^l_{IM} \cos\Big[\psi_M - \delta_{I1} \frac{\pi}{2}\Big]\, d^I_{M0}(\theta_d) \Big\} \\ + \sum_{I=1}^{2} P^d_I \sum_{M=0}^{I} \Big(T_{IM} \cos\Big[M(\phi_d - \phi) - \delta_{I1} \frac{\pi}{2}\Big] + P^\gamma_c\, T^c_{IM} \sin\Big[M(\phi_d - \phi) + \delta_{I1} \frac{\pi}{2}\Big] \Big)\, d^I_{M0}(\theta_d) \Big], \end{aligned} \tag{7}$$

where $\psi_M = M(\phi_d - \phi) + 2\phi$ and $d^I_{M0}(\theta_d)$ is a small rotation matrix for which the convention of Ref. [53] is used. The photon polarization is characterized by the degree of circular $P^\gamma_c = P^\gamma_z$ and linear $P^\gamma_l = \sqrt{(P^\gamma_x)^2 + (P^\gamma_y)^2}$ polarization, where the x-axis has been chosen in the direction of maximum linear polarization, *i.e.* $P^\gamma_x = -P^\gamma_l$ and $P^\gamma_y = 0$. The deuteron is characterized by the vector and tensor polarization components P^d_1 and P^d_2, respectively, and the orientation angles (θ_d, ϕ_d) of the orientation axis of the deuteron with respect to which the density matrix of the deuteron has been assumed to be diagonal; the elements with $m_d \neq m'_d$ will therefore vanish.

In order to express the unpolarized differential cross section and various polarization observables in terms of the t-matrix, it is appropriate to define the two quantities [50]:

$$\mathcal{V}_{IM} = \frac{\mathcal{K}}{\sqrt{3}} \sqrt{2I+1} \sum_{m_d m'_d} (-)^{1-m_d} \begin{pmatrix} 1 & 1 & I \\ m'_d & -m_d & M \end{pmatrix} \sum_{m''_d} t^*_{m''_d 1 m'_d}\, t_{m''_d 1 m_d} \,, \tag{8}$$

$$\mathcal{W}_{IM} = -\frac{\mathcal{K}}{\sqrt{3}} \sqrt{2I+1} \sum_{m_d m'_d} (-)^{1-m_d} \begin{pmatrix} 1 & 1 & I \\ m'_d & -m_d & M \end{pmatrix} \sum_{m''_d} t^*_{m''_d 1 m'_d}\, t_{m''_d -1 m_d} \,, \tag{9}$$

where the convention of Edmonds [53] is used for the Wigner $3j$-symbol. The explicit formal expressions for unpolarized differential cross section and spin asymmetries can be derived as follows [28]:

(i) The unpolarized differential cross section:

$$\frac{d\sigma_0}{d\Omega} = \mathcal{V}_{00} = \frac{\mathcal{K}}{3} \sum_{m'_d m_d} |t_{m'_d 1 m_d}|^2 \,. \tag{10}$$

(ii) The linear photon asymmetry:

$$\Sigma \, \frac{d\sigma_0}{d\Omega} = \mathcal{W}_{00} = -\frac{\mathcal{K}}{3} \sum_{m'_d m_d} t^*_{m'_d 1 m_d} \, t_{m'_d - 1 m_d} \,. \tag{11}$$

(iii) The vector target asymmetry:

$$T_{11} \, \frac{d\sigma_0}{d\Omega} = 2 \, \Im m \, \mathcal{V}_{11} = \sqrt{\frac{2}{3}} \, \mathcal{K} \, \Im m \sum_{m_d} (t^*_{m_d 1 - 1} \, t_{m_d 10} + t^*_{m_d 10} \, t_{m_d 11}) \,. \tag{12}$$

(iv) The tensor target asymmetries:

$$T_{2M} \, \frac{d\sigma_0}{d\Omega} = (2 - \delta_{M0}) \, \Re e \, \mathcal{V}_{2M} \text{ for } 0 \leq M \leq 2 \,,$$

with

$$T_{20} \, \frac{d\sigma_0}{d\Omega} = \frac{\mathcal{K}}{3\sqrt{2}} \sum_{m_d} (|t_{m_d 11}|^2 + |t_{m_d 1 - 1}|^2 - 2 \, |t_{m_d 10}|^2) \,, \tag{13}$$

$$T_{21} \, \frac{d\sigma_0}{d\Omega} = \sqrt{\frac{2}{3}} \, \mathcal{K} \, \Re e \sum_{m_d} (t^*_{m_d 1 - 1} \, t_{m_d 10} - t^*_{m_d 10} \, t_{m_d 11}) \,, \tag{14}$$

$$T_{22} \, \frac{d\sigma_0}{d\Omega} = \frac{2\mathcal{K}}{\sqrt{3}} \, \Re e \sum_{m_d} t^*_{m_d 1 - 1} \, t_{m_d 11} \,. \tag{15}$$

(v) The spin asymmetries for circularly polarized photons and vector polarized deuterons:

$$T^c_{1M} \, \frac{d\sigma_0}{d\Omega} = -(2 - \delta_{M0}) \, \Re e \, \mathcal{V}_{1M} \,, \text{ for } 0 \leq M \leq 1$$

with

$$T^c_{10} \, \frac{d\sigma_0}{d\Omega} = \frac{\mathcal{K}}{\sqrt{6}} \sum_{m_d} (|t_{m_d 11}|^2 - |t_{m_d 1 - 1}|^2) \,, \tag{16}$$

$$T^c_{11} \, \frac{d\sigma_0}{d\Omega} = -\sqrt{\frac{2}{3}} \, \mathcal{K} \, \Re e \sum_{m_d} (t^*_{m_d 1 - 1} \, t_{m_d 10} + t^*_{m_d 10} \, t_{m_d 11}) \,. \tag{17}$$

(vi) The spin asymmetries for circularly polarized photons and tensor polarized deuterons:

$$T^c_{2M} \, \frac{d\sigma_0}{d\Omega} = -(2 - \delta_{M0}) \, \Im m \, \mathcal{V}_{2M} \,, \text{ for } 0 \leq M \leq 2$$

with

$$T^c_{21} \, \frac{d\sigma_0}{d\Omega} = \sqrt{\frac{2}{3}} \, \mathcal{K} \, \Im m \sum_{m_d} (t^*_{m_d 10} \, t_{m_d 11} - t^*_{m_d 1 - 1} \, t_{m_d 10}) \,, \tag{18}$$

$$T^c_{22} \, \frac{d\sigma_0}{d\Omega} = -\frac{2\mathcal{K}}{\sqrt{3}} \, \Im m \sum_{m_d} t^*_{m_d 1 - 1} \, t_{m_d 11} \,. \tag{19}$$

Because the quantity $\mathcal{V}_{I0}$ is real according to $\mathcal{V}^*_{IM} = (-)^M \, \mathcal{V}_{I-M}$ under complex conjugation, the spin asymmetry T^c_{20} vanishes identically.

(vii) The spin asymmetries for linearly polarized photons and vector polarized deuterons:

$$T^l_{1M}\,\frac{d\sigma_0}{d\Omega} = i\,\mathcal{W}_{1M}\,, \quad \text{for} \quad -1 \le M \le 1,$$

with

$$T^l_{10}\,\frac{d\sigma_0}{d\Omega} = \sqrt{\frac{2}{3}}\,\mathcal{K}\,\Im m \sum_{m_d} t^*_{m_d 11}\,t_{m_d -11}\,, \tag{20}$$

$$T^l_{11}\,\frac{d\sigma_0}{d\Omega} = -\sqrt{\frac{2}{3}}\,\mathcal{K}\,\Im m \sum_{m_d} t^*_{m_d 1-1}\,t_{m_d -10}, \tag{21}$$

$$T^l_{1-1}\,\frac{d\sigma_0}{d\Omega} = \sqrt{\frac{2}{3}}\,\mathcal{K}\,\Im m \sum_{m_d} t^*_{m_d 11}\,t_{m_d -10}\,. \tag{22}$$

(viii) The spin asymmetries for linearly polarized photons and tensor polarized deuterons:

$$T^l_{2M}\,\frac{d\sigma_0}{d\Omega} = \mathcal{W}_{2M}\,, \quad \text{for} \quad -2 \le M \le 2,$$

with

$$T^l_{20}\,\frac{d\sigma_0}{d\Omega} = \frac{\sqrt{2}}{3}\,\mathcal{K}\,\Re e \sum_{m_d} (t^*_{m_d 10}\,t_{m_d -10} - t^*_{m_d 11}\,t_{m_d -11})\,, \tag{23}$$

$$T^l_{21}\,\frac{d\sigma_0}{d\Omega} = \sqrt{\frac{2}{3}}\,\mathcal{K}\,\Re e \sum_{m_d} t^*_{m_d 10}\,t_{m_d -11}\,, \tag{24}$$

$$T^l_{2-1}\,\frac{d\sigma_0}{d\Omega} = \sqrt{\frac{2}{3}}\,\mathcal{K}\,\Re e \sum_{m_d} t^*_{m_d 10}\,t_{m_d -1-1}\,, \tag{25}$$

$$T^l_{22}\,\frac{d\sigma_0}{d\Omega} = -\frac{\mathcal{K}}{\sqrt{3}} \sum_{m_d} t^*_{m_d 1-1}\,t_{m_d -11}\,, \tag{26}$$

$$T^l_{2-2}\,\frac{d\sigma_0}{d\Omega} = -\frac{\mathcal{K}}{\sqrt{3}} \sum_{m_d} t^*_{m_d 11}\,t_{m_d -1-1}\,. \tag{27}$$

We would like to mention that for $\theta = 0$ and π the spin asymmetries $T^c_{IM} = 0$ for $M \neq 0$ and $T^l_{IM} = 0$ for $M \neq 2$ because in that case the angle ϕ is undefined or arbitrary and, therefore, the differential cross section cannot depend on ϕ.

The deuteron spin asymmetry with respect to circularly polarized photons and the deuteron spin oriented parallel (P) and antiparallel (A) to the photon spin is related to the spin asymmetry T^c_{10} according to [54]:

$$\frac{d(\sigma^P - \sigma^A)}{d\Omega} = \sqrt{6}\,\frac{d\sigma_0}{d\Omega}\,T^c_{10}\,. \tag{28}$$

As mentioned in the Introduction, the asymmetry T^c_{10} is of special interest, because it is related to the spin asymmetry $\sigma^P - \sigma^A$ which determines the GDH sum rule [49].

The general form of the total cross section with inclusion of photon and deuteron polarization effects is obtained from Eq. (7) by integrating $d\sigma/d\Omega$ over the pion spherical angle $d\Omega$ and reads [54]:

$$\sigma(P^\gamma_l, P^\gamma_c, P^d_1, P^d_2) = \sigma_0\,\left[1 + P^d_2\,\widetilde{T}_{20}\,\frac{1}{2}(3\cos^2\theta_d - 1) + P^\gamma_c\,P^d_1\,\widetilde{T}^c_{10}\,\cos\theta_d + P^\gamma_l\,P^d_2\,\widetilde{T}^l_{22}\cos(2\phi_d)\,\frac{\sqrt{6}}{4}\sin^2\theta_d\right], \tag{29}$$

where the unpolarized total cross section σ_0 and the corresponding spin asymmetries $\sigma_0\,\widetilde{T}_{20}$, $\sigma_0\,\widetilde{T}^c_{10}$ and $\sigma_0\,\widetilde{T}^l_{22}$ are given by:

$$\sigma_0 = \int d\Omega \, \frac{d\sigma_0}{d\Omega} \,, \tag{30}$$

$$\sigma_0 \, \widetilde{T}_{20} = \int d\Omega \, \frac{d\sigma_0}{d\Omega} \, T_{20} \,, \tag{31}$$

$$\sigma_0 \, \widetilde{T}^c_{10} = \int d\Omega \, \frac{d\sigma_0}{d\Omega} \, T^c_{10} \,, \tag{32}$$

$$\sigma_0 \, \widetilde{T}^l_{22} = \int d\Omega \, \frac{d\sigma_0}{d\Omega} \, T^l_{22} \,. \tag{33}$$

2.2. The $\gamma d \to \pi^0 d$ amplitude

Next, the transition matrix elements $\mathcal{M}_{m'_d \lambda m_d}$ are calculated in the frame of time-ordered perturbation theory. The impulse approximation (IA), in which the reaction will take place only on one of the two nucleons in the deuteron leaving the other as a pure spectator, usually serves as the starting point to calculate the amplitude for electromagnetic pion production on the deuteron [16] or, in general, on a nucleus. It corresponds to a direct embedding of the elementary $\gamma N \to \pi N$ amplitudes into the two-nucleon system. In our framework, we restrict the calculation of the transition matrix elements $\mathcal{M}_{m'_d \lambda m_d}$ to IA in order to study the dependence of results for the $\gamma d \to \pi^0 d$ observables on the elementary pion photoproduction operator.

The production operator $t^d_{\gamma\pi}$ for the deuteron process is obtained from the elementary operator $t_{\gamma\pi}$ by:

$$t^d_{\gamma\pi} = t^{(1)}_{\gamma\pi} \otimes \mathbb{1}^{(2)} + \mathbb{1}^{(1)} \otimes t^{(2)}_{\gamma\pi} \,. \tag{34}$$

The upper index refers to the nucleon on which the elementary operator acts. This means that $t^d_{\gamma\pi}$ contains pure single nucleon terms. The transition $\mathcal{M}$-matrix of coherent π^0-photoproduction on the deuteron has the following form:

$$\mathcal{M}_{m'_d \lambda m_d}(\vec{k}, \vec{q}) = 2 \int \frac{d^3p}{(2\pi)^3} \, \psi^\dagger_{m'_d} \left(\vec{p} - \frac{\vec{q}}{2} \right) \times \langle \vec{p} - \vec{q} \,| \, t^{(1)}_{\gamma\pi} \, | \, \vec{p} - \vec{k} \rangle \, \psi_{m_d} \left(\vec{p} - \frac{\vec{k}}{2} \right) \,, \tag{35}$$

where $\psi_{m_d}(\vec{p})$ denotes the deuteron wave function and $t^{(1)}_{\gamma\pi}$ the elementary $\gamma N \to \pi N$ operator.

For the intrinsic part of the deuteron wave function we use the ansatz:

$$\psi_{m_d}(\vec{p}) = \sum_{L=0,2} \sum_{m_L m_S} (L m_L 1 m_S | 1 m_d) \times u_L(p) \, Y_{L m_L}(\hat{p}) \, \chi_{m_S} \, \zeta_0 \,. \tag{36}$$

The last two terms χ_{m_S} and ζ_0 denote spin and isospin wave functions, respectively. The S and D components of the deuteron wave function (DWF) are given by $u_0(p)$ and $u_2(p)$, respectively. In the present work, we compute the radial deuteron wave functions $u_L(p)$ using the realistic and high-precision Bonn full model [55].

For the elementary $\gamma N \to \pi N$ amplitude, we take the π-production operator from the unitary isobar MAID-2007 model introduced in Ref. [46]. This model is based on Born terms, ρ and ω vector-meson exchange contributions, and 13 four-star nucleon resonance excitations. It describes well the elementary $\gamma N \to \pi N$ amplitude and agrees with experimental observations very well. The MAID-2007 model is parameterized in terms of invariant amplitudes and therefore allows one to evaluate the transition deuteron amplitude in any frame of reference.

To study the uncertainties caused by the use of different elementary pion photoproduction operators in the analyses of $\gamma d \to \pi^0 d$ observables, the dynamical DMT-2001 model [47] and the χMAID-2013 model [48] are used. The DMT-2001 model is a unitary dynamical model based on a non-resonant background described by Born terms and vector-meson exchange contributions in the t-channel (ρ and ω) and the following 8 four-star nucleon resonances in the s-channel: $P_{33}(1232)$, $P_{11}(1440)$, $D_{13}(1520)$, $S_{11}(1535)$, $S_{31}(1620)$, $S_{11}(1650)$, $F_{15}(1680)$, and $D_{33}(1700)$. The DMT-2001 model describes the pion photo- and electroproduction observables in terms of photon and nucleon degrees of freedom and provides a very good description of experimental data in the near-threshold region. The χMAID-2013 model for studying pion photo- and electroproduction on the nucleon in the near-threshold region has been constructed in relativistic chiral perturbation theory and included all multipole amplitudes up to and including ℓ=4 or, in other words, G waves. This model provides a comprehensive description of the elementary process on the free nucleon up to photon energies of 170 MeV in the laboratory frame. The details of each of the used models (MAID-2007, DMT-2001, and χMAID-2013) can be found in their original works in Refs. [46–48] and therefore will not repeated here.

3. Results and discussions

In this section, we explore the sensitivity of the results for unpolarized cross sections as well as all various beam, target, and beam-target spin asymmetries of the $\gamma d \to \pi^0 d$ reaction near threshold to the elementary pion photoproduction amplitude. For this purpose, we use for the elementary reaction amplitudes three different realistic models. These models are the MAID-2007 [46], DMT-2001 [47], and χMAID-2013 [48]. For the deuteron wave function, we use the realistic and high-precision Bonn full model [55]. We discuss the energy and angular dependences of the results for these observables and give a comparison of the obtained results with the available experimental data. In all the upcoming figures, the dashed, dotted, and solid curves represent the results using MAID-2007 [46], DMT-2001 [47], and χMAID-2013 [48] models for the elementary operator, respectively.

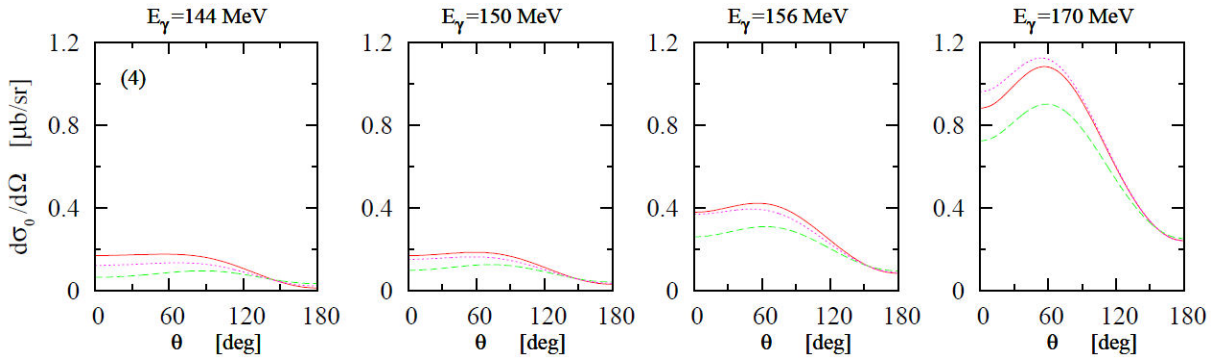

FIGURE 2. (Color online) The differential cross section for the reaction $\gamma d \to \pi^0 d$ using different elementary operators and the DWF from Bonn full potential. The dashed, dotted, and solid curves represent the results using the MAID-2007, DMT-2001, and χMAID-2013 models for the elementary operator, respectively. Results at $E_\gamma = 144$ MeV are multiplied by the factor in the parentheses.

3.1. Differential and total cross sections

First, we show in Fig. 2 the energy and angular dependences of the results for unpolarized differential cross section, $d\sigma_0/d\Omega$, using different elementary $\gamma N \to \pi N$ amplitudes. We see that the $d\sigma_0/d\Omega$ results with different elementary amplitudes are quite different especially at forward pion angles. The differences between the results with various elementary amplitudes decrease with increasing pion angle until they become very small at $\theta = 180^\circ$. When the dashed curve (MAID-2007) is compared with both the dotted (DMT-2001) and solid (χMAID-2013) curves, one can see that these differences are very obvious at forward pion angles and show up the discrepancies among elementary amplitudes. In this case, the calculated $d\sigma_0/d\Omega$ within the MAID-2007 model is smaller than those within DMT-2001 and χMAID-2013. At extreme backward pion angles, we see that the curves represent the results of $d\sigma_0/d\Omega$ using MAID-2007, DMT-2001, and χMAID-2013 are very close to each other and thus the influence of elementary operators on $d\sigma_0/d\Omega$ is negligible in this case. This means that the $d\sigma_0/d\Omega$ results are sensitive to the choice of the elementary amplitude at forward pion angles.

Figure 3 shows the results for the unpolarized total cross section, σ_0, for the reaction $\gamma d \to \pi^0 d$ as a function of the photon energy in the laboratory system, E_γ, using different elementary operators. The importance of the choice of elementary amplitude is clearly addressed when the calculation with the MAID-2007 (dashed curve) is compared to the DMT-2001 (dotted curve) and χMAID-2013 (solid curve) curves. It is very clear that the results using MAID-2007 model differ significantly from the DMT-2001 and χMAID-2013 ones. However, the σ_0 results using DMT-2001 and χMAID-2013 models are close to each other. We would like to point out that the MAID-2007 model is based on a single channel approach, whereas the DMT-2001 model is based on coupled channels. This is an important difference between both models.

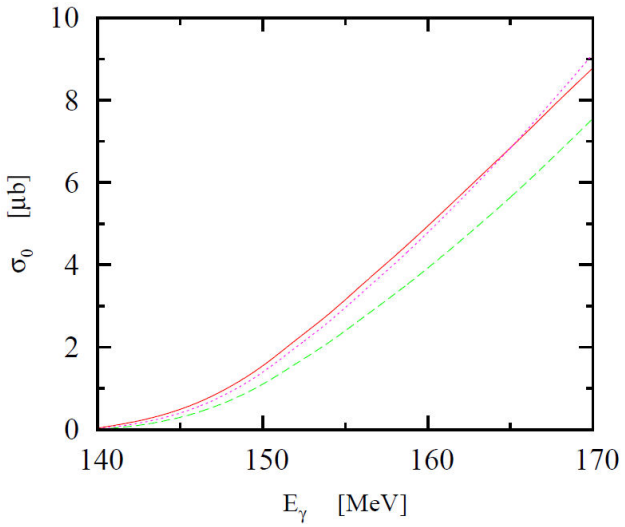

FIGURE 3. (Color online) The unpolarized total cross section for the reaction $\gamma d \to \pi^0 d$ as a function of photon lab-energy using different elementary operators and the DWF from Bonn full NN potential. Curve conventions as in Fig. 2.

3.2. Single-spin asymmetries

Now, we focus our attention on the single-spin asymmetries of polarized photons (Σ) or polarized deuterons (T_{11}, T_{20}, T_{21}, and T_{22}) for $\vec{\gamma} d \to \pi^0 d$ and $\gamma \vec{d} \to \pi^0 d$, respectively. We present in Fig. 4 the results for the linear photon asymmetry Σ at different photon lab-energies as a function of emission pion angle θ in the γd c.m. frame. In general, one can see the results for Σ remain same qualitatively but quantitatively slightly changed. Figure 4 shows that the photon Σ-asymmetry has dominately negative values in the photon energy domain of the present work. One displays also that the Σ-asymmetry decreases with increasing pion scattering angle until a minimum close to $\theta \simeq 130^\circ$ at $E_\gamma = 144$ MeV is reached. This minimum is shifted towards lower pion angles with increasing the photon lab-energy. Then the photon asymmetry Σ increases with increasing pion angle until it reaches zero at $\theta = \pi$. It is also noticeable from Fig. 4 that the photon asymmetry Σ vanishes at $\theta = 0^\circ$ and 180°, because in that case the differential cross section cannot depend on the azimuthal angle ϕ, since at $\theta = 0$ and π the angle ϕ

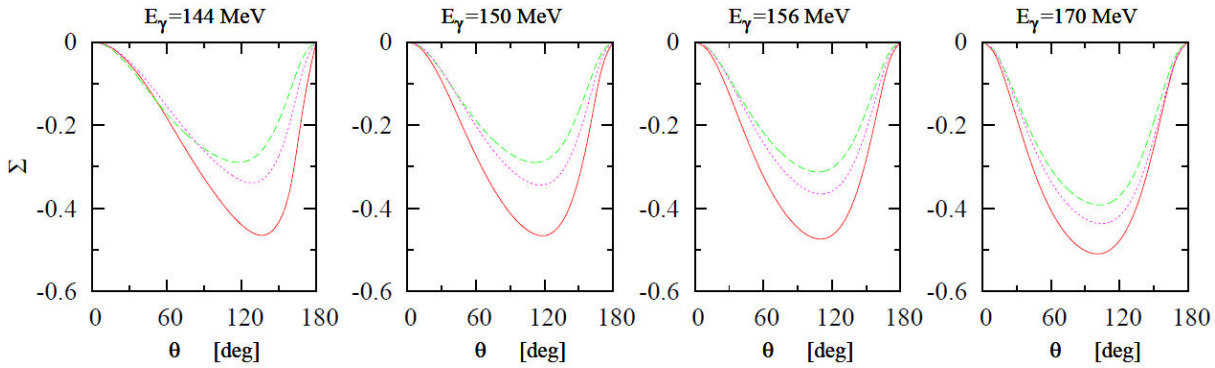

FIGURE 4. (Color online) Same as in Fig. 2 but for the photon Σ-asymmetry with linearly polarized photons and unpolarized deuterons.

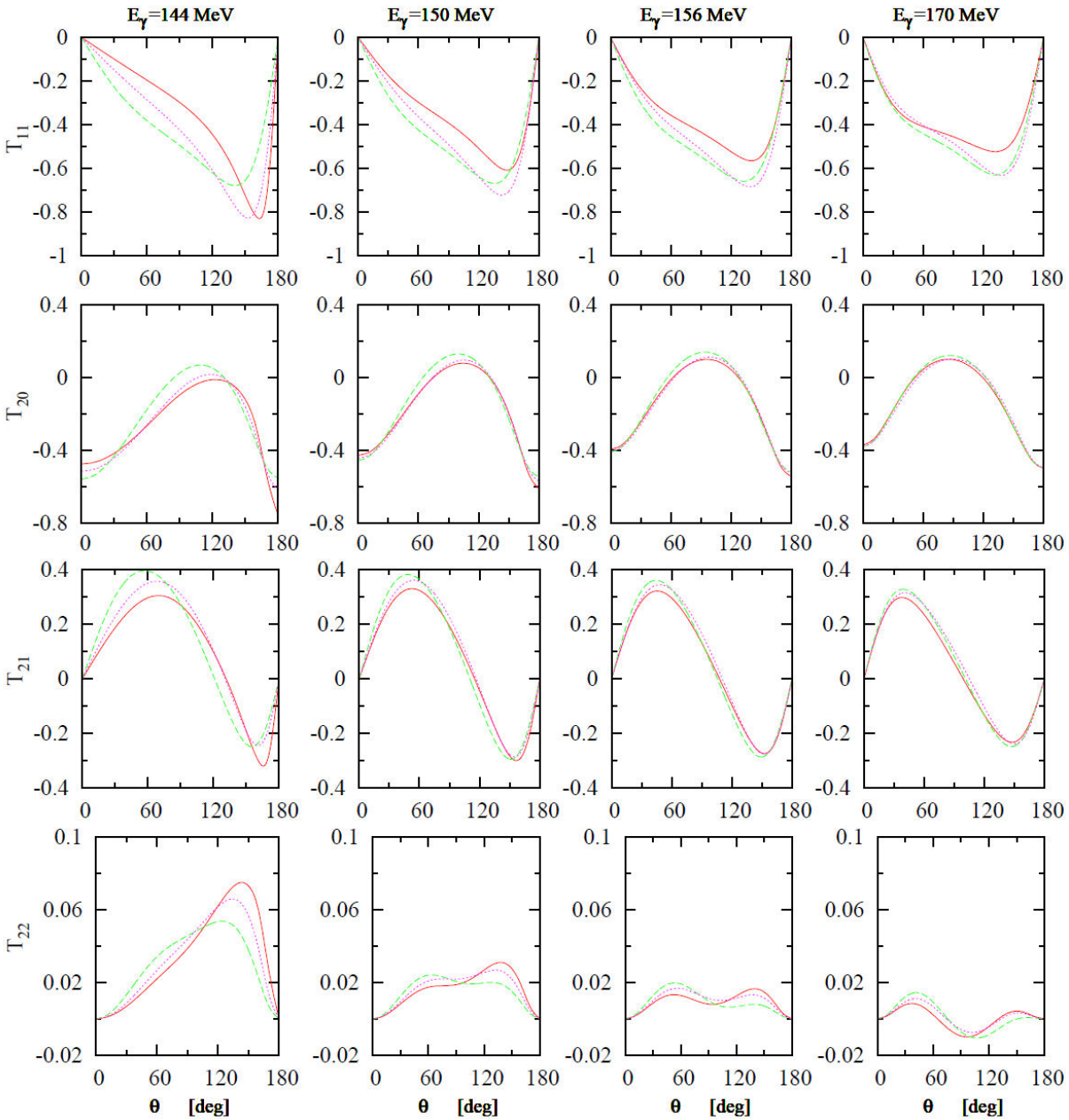

FIGURE 5. (Color online) Same as in Fig. 2 but for the deuteron asymmetries with vector T_{11} and tensor T_{2M} ($M = 0, 1, 2$) polarized deuterons and unpolarized photons.

is undefined or can be arbitrary. At extreme forward and backward emission pion angles, one notes that the photon Σ-asymmetry is relatively small in comparison to the results when θ varies from 60° to 150°.

We found that the asymmetry Σ is sensitive to the elementary amplitude, especially in the peak region where sizeable differences are obtained in the pion angle range from 60° to 150°. It has a minimal value around $\theta \simeq 135^\circ$ in the case of χMAID-2013 (solid curve) and it is shifted towards lower pion angles in the case of DMT-2001 (dotted curve) and MAID-2007 (dashed curve). It is also very obvious that the computations with different elementary amplitudes are quite different with, in absolute size, a larger Σ-asymmetry predicted using χMAID than the ones obtained with DMT and MAID models. This discrepancy shows up the differences among elementary pion photoproduction operators and means that Σ is very sensitive to the choice of the elementary amplitude, in particular in the vicinity of the peak.

For polarization observables with polarized deuteron targets and unpolarized photon beams, we present in Fig. 5 the sensitivity of the results for the vector T_{11} and tensor T_{2M} ($M = 0,1,2$) deuteron spin asymmetries for the reaction $\gamma \vec{d} \to \pi^0 d$ to the choice of elementary pion photoproduction amplitude. We see that the results for T_{11} asymmetry exhibit qualitatively similar behaviors for different elementary pion photoproduction operators. The T_{11} asymmetry is sensitive to the imaginary parts of the scattering amplitudes and its values vanish identically at $\theta = 0$ and π. This asymmetry depends on the relative phase of the matrix elements as can be seen from Eq. (12). It would vanish for a constant overall phase of the t-matrix. One can also see that the results using different elementary operators are quantitatively rather different even at forward and backward pion angles. This discrepancy displays the differences among elementary pion photoproduction operators which means that the T_{11}-asymmetry is sensitive to the choice of the elementary amplitude.

The results for tensor deuteron spin asymmetries T_{2M} ($M = 0,1,2$) are also shown in Fig. 4. In general, we see that the results for these asymmetries at the lowest photon energy, $E_\gamma = 144$ MeV, are rather different than the results at higher photon energies, especially in the case of T_{22} asymmetry. The results for T_{20} and T_{21} asymmetries using various elementary amplitudes exhibit qualitatively, but not quantitatively, similar behaviors. One can see that the results using different elementary operators are quantitatively rather different, which means that these spin asymmetries are slightly sensitive to the choice of the elementary amplitude. When the photon energy increases, we see that the curves represent the results of T_{20} and T_{21} using various elementary amplitudes are close to each other and thus the influence of elementary operators on T_{20} is small in this case. The T_{22} asymmetry indicates at photon energies greater than 144 MeV that it has an oscillatory shape. In contrast to the T_{20} and T_{21} cases, we find that the results for T_{22} asymmetry using different elementary amplitudes exhibit qualitatively and quantitatively different behaviors and show up the sensitivity of its results to the elementary amplitude.

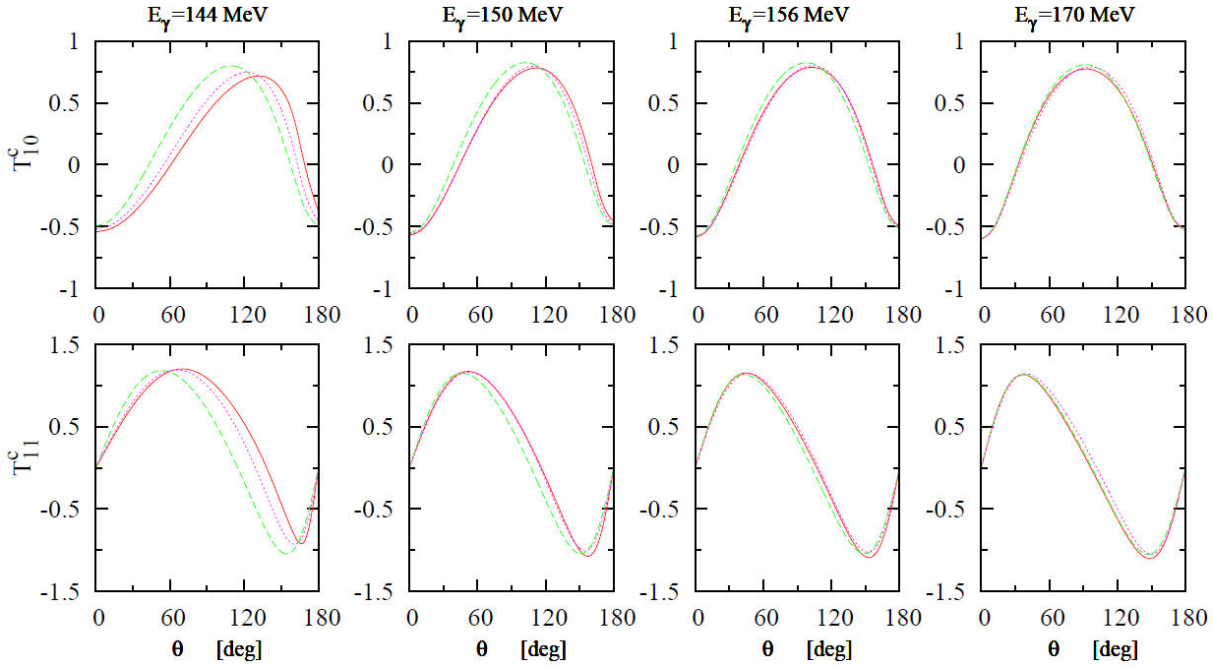

FIGURE 6. (Color online) Same as in Fig. 2 but for the beam-target double-spin asymmetries with circularly polarized photons and vector polarized deuterons.

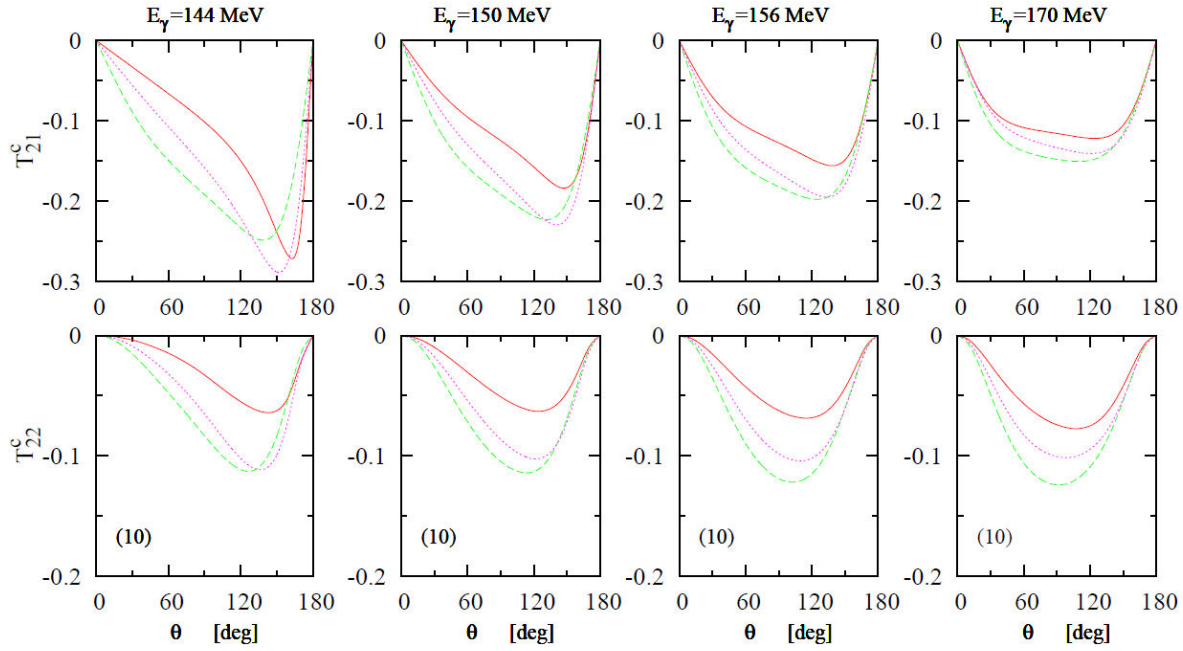

FIGURE 7. (Color online) Same as in Fig. 2 but for the beam-target double-spin asymmetries with circularly polarized photons and tensor polarized deuterons. Results for the T^c_{22} asymmetry are multiplied by the factor in the parentheses.

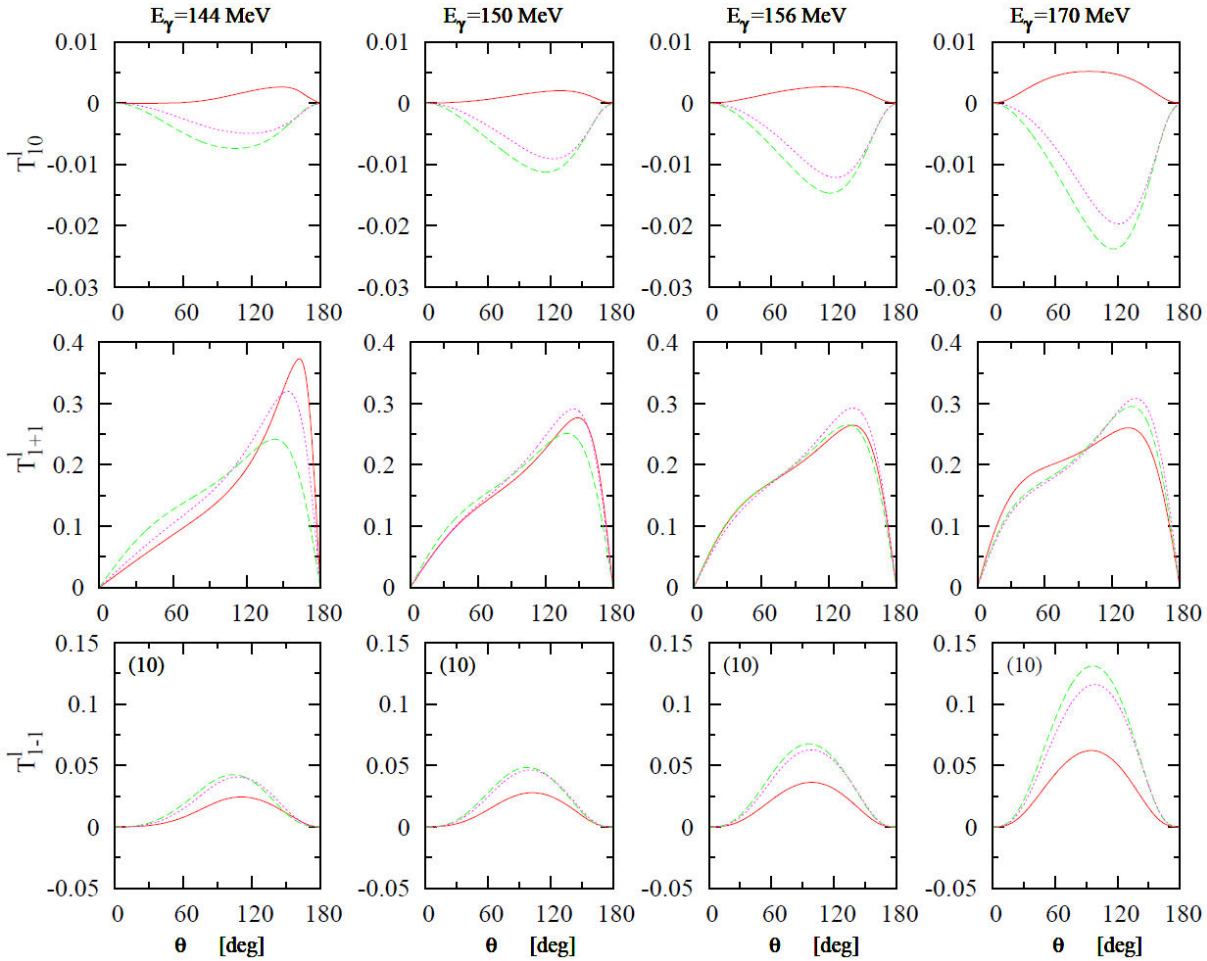

FIGURE 8. (Color online) Same as in Fig. 2 but for the beam-target double-spin asymmetries with linearly polarized photons and vector polarized deuterons. Results for the T^l_{1-1} asymmetry are multiplied by the factor in the parentheses.

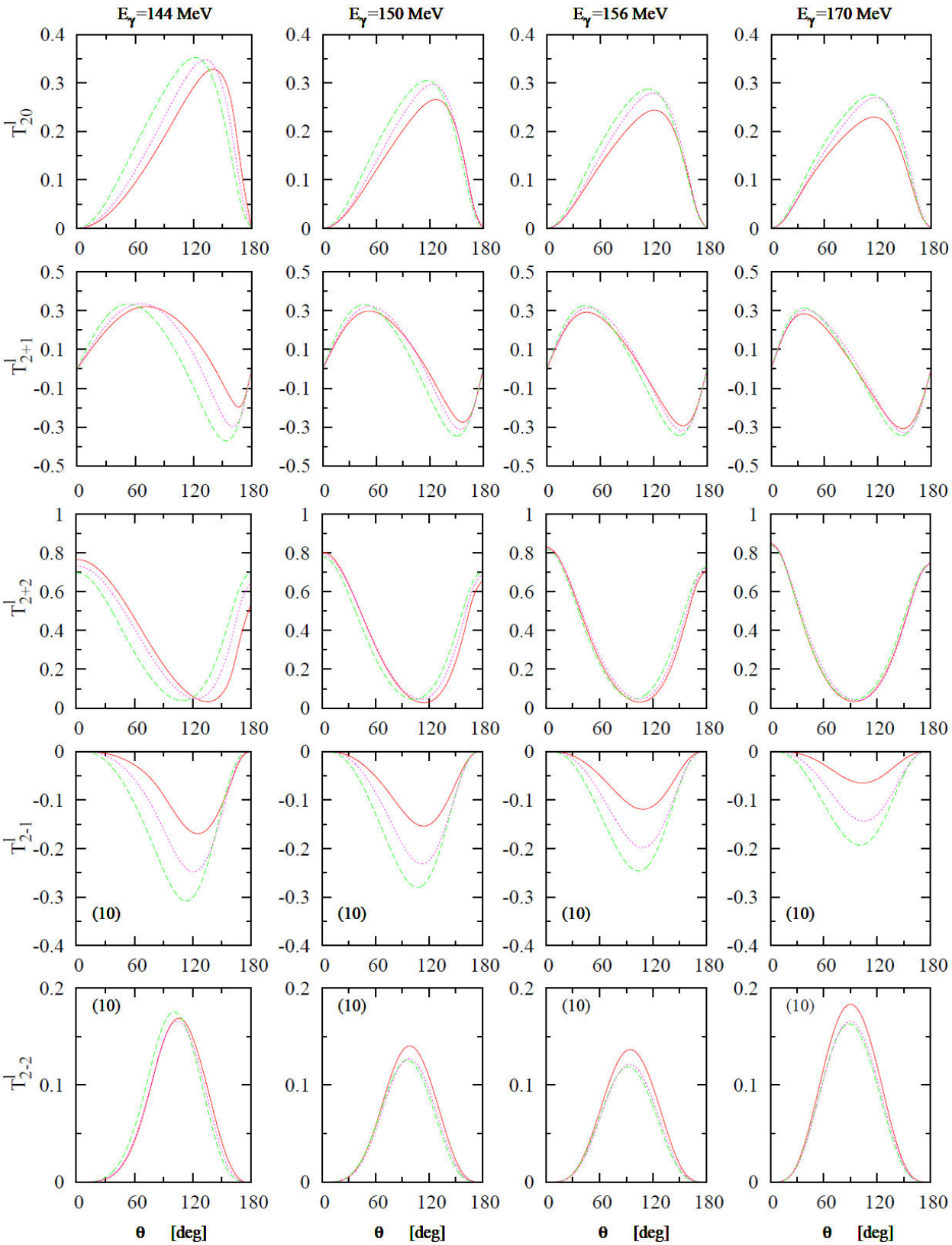

FIGURE 9. (Color online) Same as in Fig. 2 but for the beam-target double-spin asymmetries with linearly polarized photons and tensor polarized deuterons. Results for the T^l_{2-1} and T^l_{2-2} asymmetries are multiplied by the factor in the parentheses.

3.3. Beam-target double-spin asymmetries

Here, we report the numerical results for the beam-target double spin asymmetries for $\vec{\gamma}\vec{d} \to \pi^0 d$ reaction near threshold. We start with the results for T^c_{10} and T^c_{11} asymmetries with circular polarized photons and vector polarized deuterons as shown in Fig. 6 as functions of pion angle in the γd c.m. frame at the same photon lab-energies as mentioned before in the case of single-spin asymmetries. We see that the results for T^c_{10} and T^c_{11} at different photon lab-energies remain same qualitatively but quantitatively slightly changed. The T^c_{10} and T^c_{11} asymmetries behave the same as T_{20} and T_{21} ones, respectively. Figure 6 displays that the T^c_{10} asymmetry has values between -1 and 1. It begins negative at $\theta = 0^\circ$ and increases with increasing pion angle until a maximum value at $\theta \simeq 90^\circ$. Then, it rapidly falls down to negative values when increasing the pion angles. The maximum value of T^c_{10} is shifted towards higher pion angles at $E_\gamma = 144$ MeV. As mentioned in the Introduction, the spin asymmetry T^c_{10} determines the GDH sum rule [49]. The T^c_{11} results vanish at $\theta = 0$ and π and indicate that it has an oscillatory shape. The T^c_{10} and T^c_{11} results using different elementary operators are quantitatively rather different at the lowest photon energy, which means that these asymmetries are sensitive to the choice of the elementary amplitude close to threshold. By increasing photon energies, the curves represent the results of T^c_{10} and T^c_{11} using different pion production amplitudes are close to each other and thus a small dependence of these asymmetries on the elementary operators is obtained.

Figure 7 shows the results for the beam-target double spin asymmetries T^c_{21} and T^c_{22} for circularly polarized photons and tensor polarized deuterons. A quick glance reveals that the results for T^c_{21} and T^c_{22} are negative and vanish at θ=0 and π. In contrast to the vector spin asymmetries T^c_{10} and T^c_{11}, it is obvious from Fig. 7 that the tensor spin asymmetries T^c_{21} and T^c_{22} are much more sensitive to the choice of elementary amplitude. Figure 7 shows also that the sensitivity of T^c_{21} and T^c_{22} results to the elementary pion photoproduction amplitude is very important, especially in the pion angle range between 30° and 120°.

In Fig. 8 we present our results for T^l_{10}, T^l_{1+1}, and T^l_{1-1} double spin asymmetries with longitudinal polarized photons and vector polarized deuterons. In general, we see that these double spin asymmetries are sensitive to the elementary amplitude, especially in the pion angle range between 30° and 150°. The asymmetry T^l_{10} is smaller than the other ones and it differs in size between the results with different elementary amplitudes. This emphasizes the very important dependence of the T^l_{10} results on the elementary amplitude. As discussed in Refs. [31, 38], the vector asymmetries T^l_{1M} are considerably small for π^0 production near threshold. Figure 8 displays also that the difference between the results for T^l_{10} and T^l_{1-1} asymmetries using χMAID-2013 model and both DMT-2001 and MAID-2007 increases with increasing photon lab-energy, which indicates that these spin asymmetries are very sensitive the choice of the elementary $\gamma N \to \pi N$ amplitude.

The results for the beam-target double spin asymmetries T^l_{20}, T^l_{2+1}, T^l_{2+2}, T^l_{2-1}, and T^l_{2-2} with longitudinal polarized photons and tensor polarized deuterons are shown in Fig. 9. We see that these spin asymmetries are also affected by the choice of various elementary amplitudes, especially at photon energies close to threshold. The sensitivity of the results for these asymmetries to the elementary amplitude is very obvious at the lowest photon energy, $E_\gamma = 144$ MeV, and decreases with increasing photon energy. This sensitivity is much more obvious in the case of T^l_{20} and T^l_{2-1} asymmetries since the differences between the results with various elementary operators are significant, in particular in the peak region. The $T^l_{2\pm2}$ asymmetries are sensitive to both the real and the imaginary parts of the scattering amplitudes.

Figure 10 shows the results for the beam-target double-spin asymmetries $\sigma_0 \widetilde{T}_{20}$, $\sigma_0 \widetilde{T}^c_{10}$ and $\sigma_0 \widetilde{T}^l_{22}$ of the total cross section as functions of the photon lab-energy. We see that the results for these asymmetries with different elementary amplitudes are quite different. The differences between the

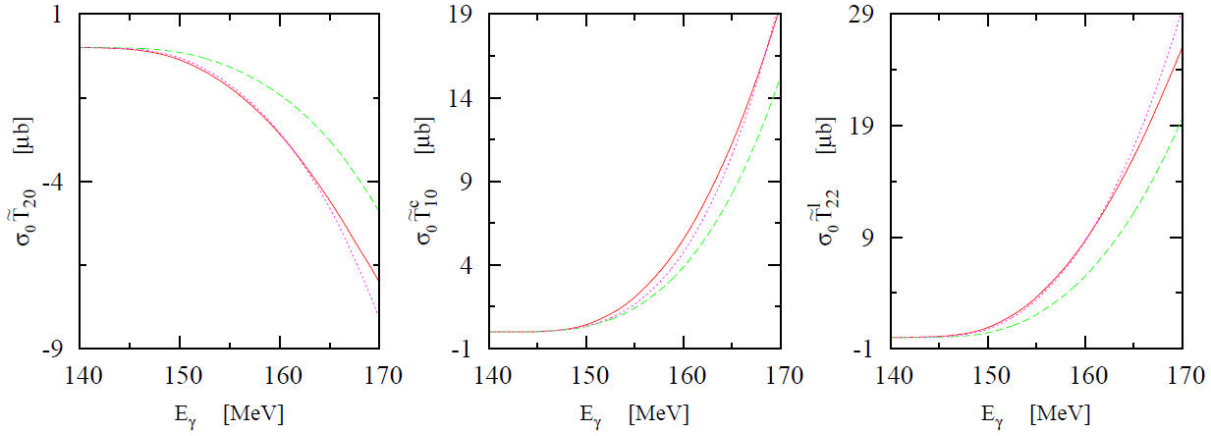

FIGURE 10. (Color online) Same as in Fig. 3 but for the beam-target double-spin asymmetries $\sigma_0 \widetilde{T}_{20}$, $\sigma_0 \widetilde{T}^c_{10}$ and $\sigma_0 \widetilde{T}^l_{22}$ of the total cross section.

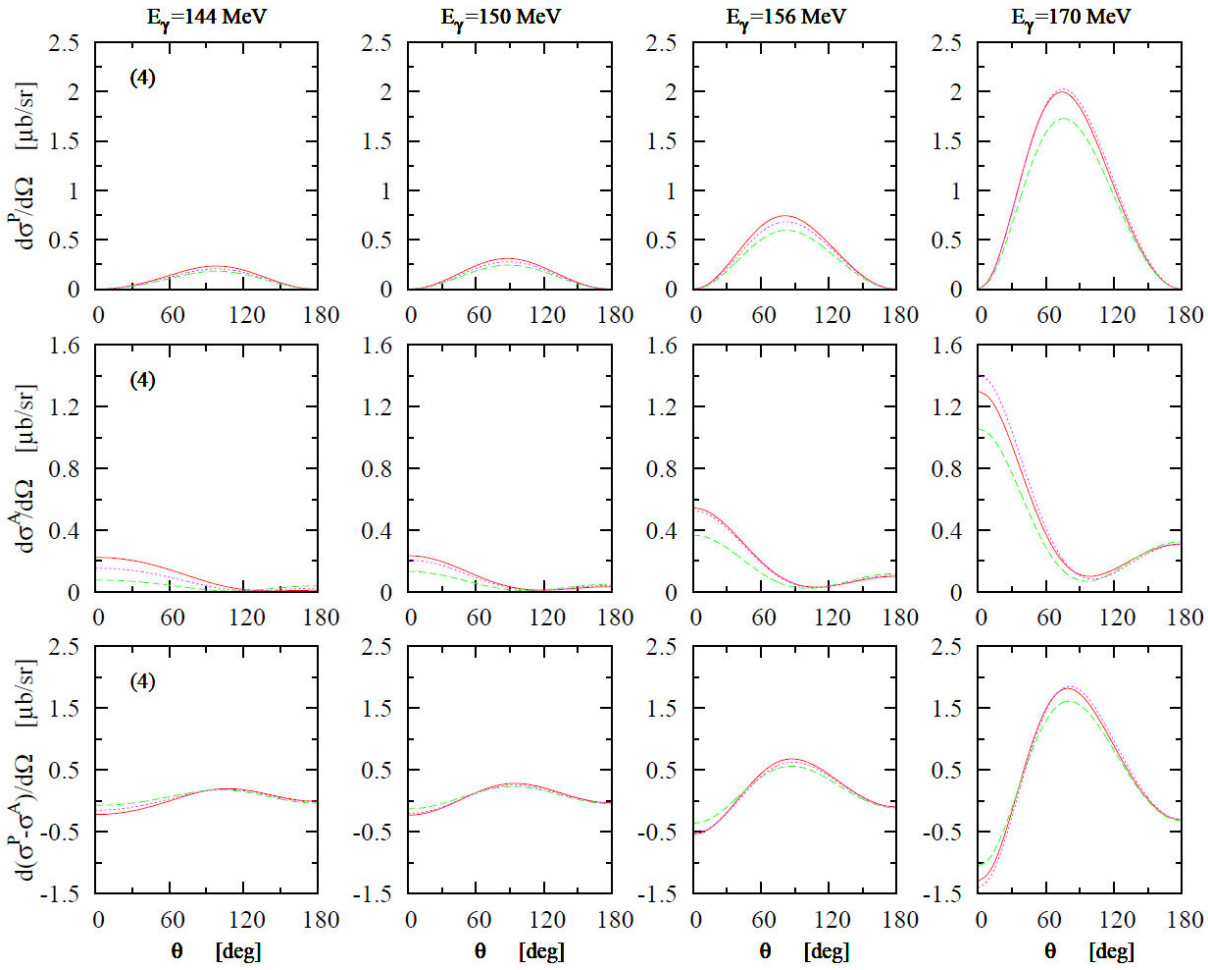

FIGURE 11. (Color online) Same as in Fig. 2 but for the doubly polarized differential cross sections for parallel (upper part) and antiparallel (middle part) spins of photon and deuteron and their difference (lower part). Results at $E_\gamma = 144$ MeV are multiplied by the factor in the parentheses.

results with various elementary amplitudes increase with increasing photon lab-energy. When the dashed curve (MAID-2007) is compared with both the dotted (DMT-2001) and solid (χMAID-2013) curves, one can see that these differences are obvious and show up the discrepancies among elementary amplitudes. The calculated $\sigma_0 \widetilde{T}_{20}$, $\sigma_0 \widetilde{T}^c_{10}$, and $\sigma_0 \widetilde{T}^l_{22}$ within MAID-2007 model is, in absolute size, smaller than those within DMT-2001 and χMAID-2013. At photon energies close to threshold, we see that the curves represent the results of $\sigma_0 \widetilde{T}_{20}$, $\sigma_0 \widetilde{T}^c_{10}$, and $\sigma_0 \widetilde{T}^l_{22}$ using MAID-2007, DMT-2001, and χMAID-2013 models are close to each other and thus the influence of elementary operator on these spin asymmetries is negligible in this case.

3.4. Helicity-dependent cross sections and E-asymmetry

Next, we present in Fig. 11 the results for the doubly polarized differential cross sections for parallel (upper part) and antiparallel (middle part) spins of photon and deuteron as functions of pion angle in the c.m. frame at various photon lab-energies using different elementary amplitudes. These polarized differential cross sections are given by

$$\frac{d\sigma^P}{d\Omega} = \frac{d\sigma_0}{d\Omega}\left[1 + \frac{1}{\sqrt{2}}T_{20} + \sqrt{\frac{3}{2}}T^c_{10}\right], \qquad (37)$$

$$\frac{d\sigma^A}{d\Omega} = \frac{d\sigma_0}{d\Omega}\left[1 + \frac{1}{\sqrt{2}}T_{20} - \sqrt{\frac{3}{2}}T^c_{10}\right]. \qquad (38)$$

In Fig. 11 we also present an important physical observable which is the difference $d(\sigma^P - \sigma^A)/d\Omega$ (lower part) that has a direct relation with the GDH sum rule [49]. The results displayed show the contribution of each $d\sigma^P/d\Omega$ and $d\sigma^A/d\Omega$ on the difference. Since their values have opposite behavior with increasing θ, we can see that the difference has negative values at small pion angles $0^\circ < \theta < 30^\circ$ because of $d\sigma^A/d\Omega$ has the larger contribution in this range of pion angles. Thereafter, for θ ranges between 30° and 90°, $d(\sigma^P - \sigma^A)/d\Omega$ starts to increase and behaves the same as $d\sigma^P/d\Omega$. For $\theta > 90^\circ$, the values of $d(\sigma^P - \sigma^A)/d\Omega$ start to decrease due to $d\sigma^A/d\Omega$ which has larger contribution again.

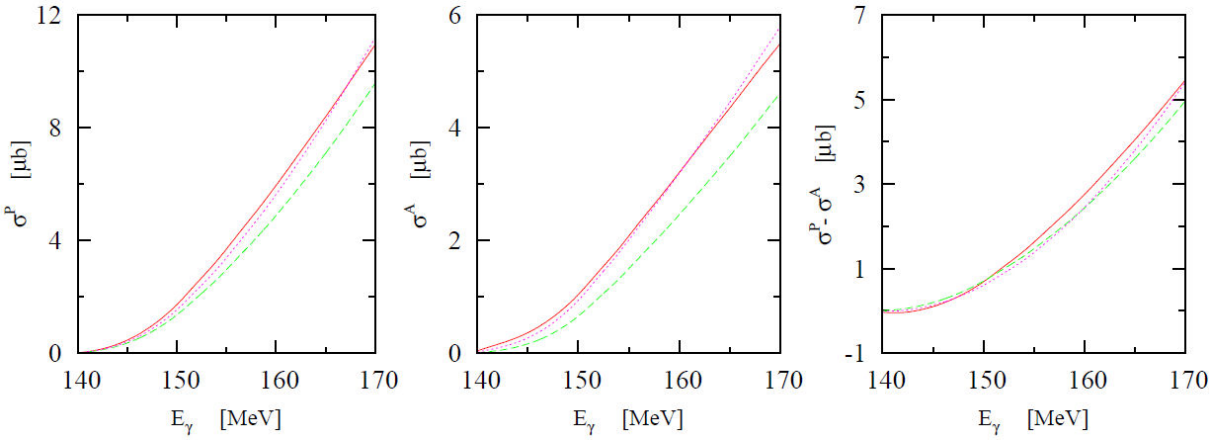

FIGURE 12. (Color online) Same as in Fig. 3 but for the doubly polarized total cross sections for parallel (left panel) and antiparallel (middle panel) spins of photon and deuteron and their difference (right panel).

We would like to mention that the threshold region is dominated by the pion production with spin $1/2$, which makes the antiparallel term $d\sigma^A/d\Omega$ larger than the parallel one $d\sigma^P/d\Omega$. The estimated values of $d(\sigma^P - \sigma^A)/d\Omega$ close to threshold at $E_\gamma = 144$ MeV are rather small compared to their values at higher energies under consideration.

As for the $d\sigma^P/d\Omega$ results (upper part in Fig. 11), we observe that the results are sensitive to the choice of elementary amplitude at the peak region since we obtain smaller values using MAID-2007 than using DMT-2001 and χMAID-2013. At extreme forward and backward pion angles, similar results are obtained and the sensitivity of $d\sigma^P/d\Omega$ results to the elementary amplitude is negligible. In the case of $d\sigma^A/d\Omega$ results (middle part in Fig. 11), we see that the influence of $d\sigma^A/d\Omega$ on the elementary amplitude is similar to the case of unpolarized differential cross section. One can see that the differences among $d\sigma^A/d\Omega$ results using different elementary amplitudes are very obvious at forward pion angles and the calculation within the MAID-2007 is smaller than those within DMT-2001 and χMAID-2013 but provides similar results at extreme pion backward angles. This discrepancy shows up the differences among elementary amplitudes. The computations of the differential spin asymmetry with respect to circularly polarized photons and oriented deuterons, $d(\sigma^P - \sigma^A)/d\Omega$, (lower part in Fig. 11) shows that the sensitivity to the choice of elementary amplitude is also important in the peak position. This means that the difference $d(\sigma^P - \sigma^A)/d\Omega$ is also sensitive to the choice of the elementary amplitude.

Figure 12 shows the results for the helicity-dependent total cross sections for the $\vec{\gamma}\vec{d} \to \pi^0 d$ reaction as functions of photon lab-energies using different elementary amplitudes. Results are displayed as follows: (left panel) total cross section σ^P for circularly polarized photons on a deuteron target with spin parallel to the photon spin; (middle panel) σ^A, the same for antiparallel spins of photon and deuteron; (right panel) spin asymmetry $\sigma^P - \sigma^A$. We see that the cross sections σ^P and σ^A as well as the deuteron spin asymmetry $\sigma^P - \sigma^A$ present similar behaviors for all elementary amplitudes used in the present work. Compared the calculation with the MAID-2007 (dashed curve) to the DMT-2001 (dotted curve) and χMAID-2013 (solid curve) ones, we clearly address the importance of the choice of elementary amplitude. We see that the results using MAID-2007 model differ from the DMT-2001 and χMAID-2013 ones. We also find that the results for $\sigma^P - \sigma^A$ starts out negative due to the E_{0+} multipole, which is dominant in the threshold region. The influence of elementary amplitude is important in σ^P, σ^A, and $\sigma^P - \sigma^A$. We would like to emphasize here that several experiments to measure the deuteron spin asymmetry $\sigma^P - \sigma^A$ are presently underway [3, 8, 9].

During the recent years, there is a considerable interest in experiments [1–7] to measure the double polarization observable E for the $\vec{\gamma}\vec{d} \to \pi^0 d$ reaction. This asymmetry is given by

$$E(\theta) = \frac{d(\sigma^A - \sigma^P)/d\Omega}{d(\sigma^A + \sigma^P)/d\Omega} = \frac{d(\sigma^A - \sigma^P)/d\Omega}{2d\sigma_0/d\Omega}\,. \qquad (39)$$

In Fig. 13 we present the results for E-asymmetry as a function of the emission pion angle θ in the γd c.m. frame at four fixed values of the incident photon lab-energy. We see that the E-asymmetry has qualitatively a similar behavior for all incident photon lab-energies considered. Its maximum equals unity at $\theta = 0^\circ$ and 180°. The curves begin with unity and decrease as the pion angle increases until a minimum value at $\theta \simeq 120^\circ$ is reached. Then, it increases again to unity. The minimum value is shifted towards lower pion angles with increasing E_γ. The negative values in the E-asymmetry come mainly from higher positive contribution in $d\sigma^P/d\Omega$. As mentioned in Refs. [22, 34], the beam-target double polarization E-asymmetry is an excellent observable to test any weakness in the underlying elementary pion photoproduction model. Figure 13 shows that the helicity E-asymmetry is sensitive to the choice of the elementary $\gamma N \to \pi N$ amplitude at incident photon lab-energies close to threshold. When the photon energy increases, we see that the sensitivity of the results for E-asymmetry to the choice of the pion photoproduction operator is rather small.

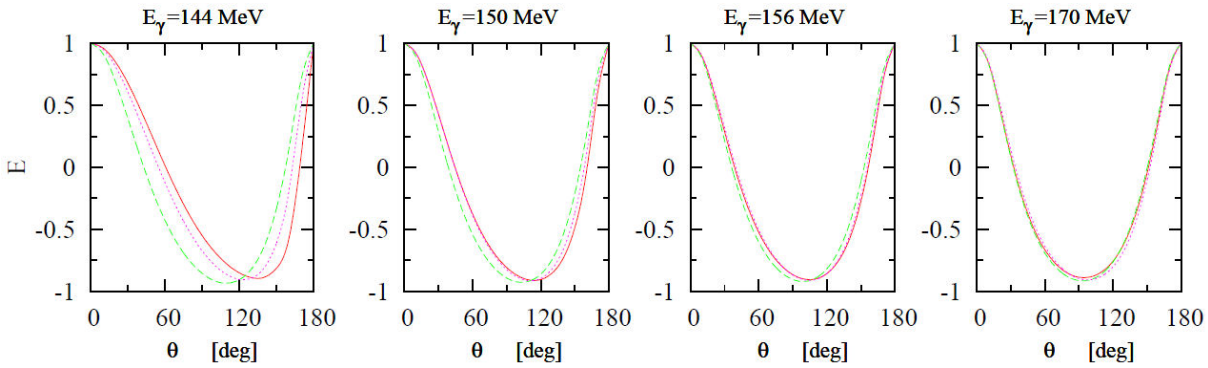

FIGURE 13. (Color online) Same as in Fig. 3 but for the double polarization E-asymmetry.

3.5. Comparison with experimental data

We close this section by comparing our results with the available experimental data. In fact, several experiments to measure both single and double polarization observables for coherent π^0-photoproduction on the deuteron are presently underway. Unfortunately, no data are currently available for these polarization observables in the kinematic region under consideration in the present work and therefore we cannot make a comparison to experimental data for polarization observables. Thus, in the present work we compare the calculated results for the unpolarized differential cross section with the available data.

Figure 14 shows a comparison between our results for the unpolarized differential cross section $d\sigma_0/d\Omega$ at two values of photon lab-energies ($E_\gamma = 151.4$ and 171.8 MeV) and the experimental data from TAPS [4]. One readily sees, that the estimated results for $d\sigma_0/d\Omega$ using different elementary amplitudes underestimate the experimental data at backward pion angles. The results with the χMAID-2013 model (solid curve) are the nearest one to the experimental data in this case. At forward pion angles and $E_\gamma = 151.4$ MeV, an overestimation of the results using χMAID-2013 and DMT-2001 elementary amplitudes is found. But the results for $d\sigma_0/d\Omega$ using MAID-2007 model underestimate the last three data points at high angles. At $E_\gamma = 171.8$ MeV and for forward pion angles, a good agreement with the experimental data is also obtained. In this case, the shape given by MAID model is consistent with data lacking only in strength. We would like to mention that the elementary operators considered in the present work use some values of resonance photocouplings which especially in case of neutron are not yet well understood, and fitting these values to the data could improve the agreement between theory and experiment.

We would like to point out that even at the PWIA level studied in the present work, there are also uncertainties due to the deuteron wave function, since one is involving large momentum components of the deuteron. Therefore, in Fig. 15 we present results for $d\sigma_0/d\Omega$ using different deuteron wave functions in comparison with the experimental data from TAPS [4]. For this purpose, we use the deuteron wave functions of the Bonn full [55] (solid curve), CD-Bonn [56] (dashed curve), and Paris [57] (dotted curve) NN potentials. These potentials are exceedingly employed for numerical es-

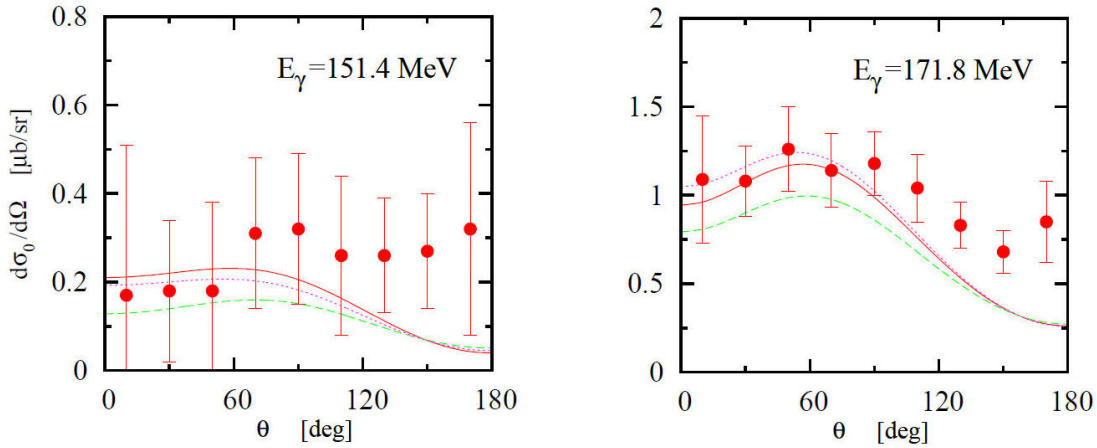

FIGURE 14. (Color online) The unpolarized differential cross section for $\gamma d \to \pi^0 d$ in comparison with the experimental data from TAPS [4]. Curve conventions as in Fig. 2.

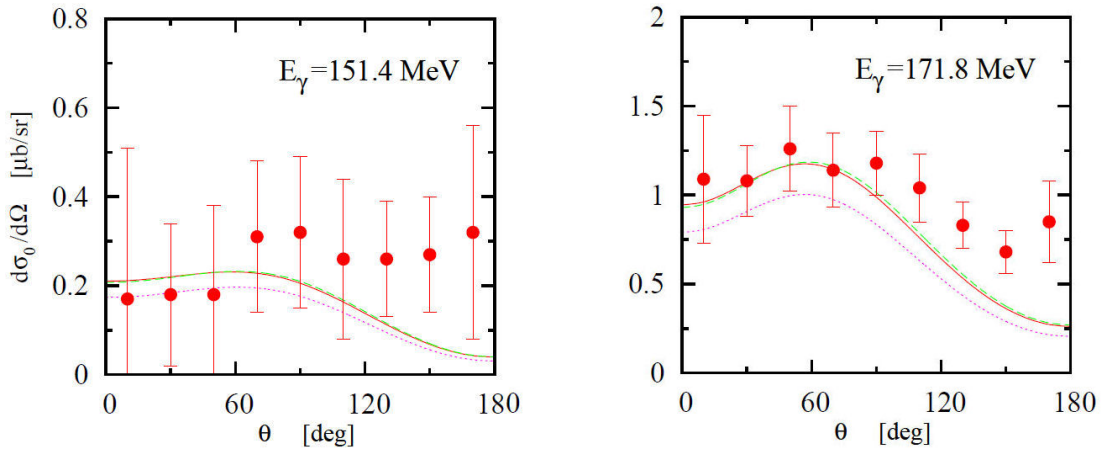

FIGURE 15. (Color online) The unpolarized differential cross section for $\gamma d \to \pi^0 d$ using χMAID-2013 elementary amplitude in comparison with the experimental data from TAPS [4]. The dotted, dashed, and solid curves represent the results using the Paris, CD-Bonn, and Bonn-full NN potentials for the deuteron wave function, respectively.

timations of electromagnetic reactions on the deuteron, give a precise characterization of the NN scattering data and phase shifts, and used to characterize the range of the NN interaction.

It is clear from Fig. 15 that the results using the deuteron wave function of the Paris potential is smaller than those using CD-Bonn and Bonn full potentials. At $E_\gamma = 151.4$ MeV, we note an overestimation of the results using CD-Bonn and Bonn full potentials at $\theta < 60^\circ$, whereas a good agreement with the experimental data using the Paris potential is obtained in this case. On the contrary, a good agreement between the results using CD-Bonn and Bonn full potentials and the experimental data is obtained at $E_\gamma = 171.8$ MeV and forward pion angles. The results using the Paris potential underestimate the experimental data in this case. At backward pion angles, we see that the results using various NN potentials underestimate the experimental data. The origin of the differences obtained using various realistic deuteron wave functions maybe due to the tensor force between two nucleons. It is well-known that a practical measure for the strength of the tensor-force component contained in a nuclear potential is the predicted D-state probability of the deuteron, P_D (see, for example, Refs. [58,59]). The P_D values for the NN potentials used in this work are 4.85% for CD-Bonn, 4.25% for Bonn full, and 5.77% for Paris. The difference in these values of P_D is related to the different tensor part of the NN potentials. The dependence of the $\gamma d \to \pi^0 d$ and $ed \to e'd'$ observables on the D-state component of the deuteron wave function was investigated in Refs. [20] and [60], respectively. It was found that the D-wave contribution becomes visible at backward scattering angles.

The obtained discrepancies between our estimations for $d\sigma_0/d\Omega$ and the experimental data can be attributed to the neglected contributions from two-body effects in the transition $\mathcal{M}$-matrix. It was found in Refs. [16, 61] that the influence of intermediate first-order pion rescattering and the two-loop diagram which includes πN and NN rescattering in the intermediate state are very important at photon energies near threshold. In addition, the meson-exchange current effects were found to be quite significant for coherent π^+ photoproduction on ^{3}He in Ref. [62].

From the preceding discussions it is apparent that the choice of the elementary amplitude has a visible effect on unpolarized cross sections as well as on various beam, target, and beam-target spin asymmetries in the $\gamma d \to \pi^0 d$ reaction near threshold. Summarizing, we can say that the MAID-2007 model provides different predictions for all possible observables in $\gamma d \to \pi^0 d$ than the χMAID-2013 and DMT-2001 models and that these observables provide excellent test object for different elementary operators.

4. Summary and outlook

The main topic of this article was to discuss theoretical uncertainties in the analyses of $\gamma d \to \pi^0 d$ observables near threshold due to the use of elementary $\gamma N \to \pi N$ amplitudes using a model which is based on time-ordered perturbation theory. As input we have used the realistic MAID-2007 model [46] for the elementary amplitude and the high-precision Bonn full NN potential [55] for the deuteron wave function. We have presented results for the unpolarized differential and total cross sections as well as for all possible beam, target, and beam-target spin asymmetries of the differential and total cross sections in the photon energy region from near π-threshold to 170 MeV. In particular, we have studied the sensitivity of the calculated results to the choice of elementary pion photoproduction amplitude. For this purpose, we have used in addition to the MAID-2007 model [46] the realistic elementary amplitudes from DMT-2001 [47] and χMAID-2013 [48] models. We have also compared our calculations with the available experimental data.

We have found that the estimations of the uncertainty on the $\gamma d \to \pi^0 d$ observables show important sensitivity to the modeling of the elementary $\gamma N \to \pi N$ operator. In

many cases the deviation among results obtained using different elementary amplitudes is very large. It may be possible that the background contribution from the crossed nucleon pole amplitude plays a significant role in the results presented in this work, because the relative importance of direct and crossed nucleon pole amplitudes grows below the Δ-resonance region. The direct nucleon pole amplitude always interferes constructively with the Δ-resonance one, whereas the crossed nucleon pole amplitude interferes constructively for energies below the Δ-resonance region. The differences found in the predictions of $\gamma d \to \pi NN$ observables [34–39] using different elementary operators are also seen here in the results for $\gamma d \to \pi^0 d$ observables. The calculated results for the unpolarized differential cross section using different elementary amplitudes are compared with the experimental data from TAPS [4]. A satisfactory agreement between theory and experiment is obtained only at forward pion angles. At backward pion angles, the calculations underestimate the experimental data and a disagreement is obtained.

The results presented above highlight the sensitivity of $\gamma d \to \pi^0 d$ observables to the choice of pion photoproduction amplitude. The obtained differences in the numerical results for $\gamma d \to \pi^0 d$ observables with various elementary operators can be attributed to the numerical account for the off-shell effects when the elementary nucleon amplitude is embedded into the deuteron process. In fact, it is difficult to give precise quantitative account for these off-shell effects, because the equivalence existing in the on-shell $\gamma N \to \pi N$ operator is broken in deuteron calculations when one nucleon or both of them are off their mass shells.

In summary, we conclude that the calculated results are of particular interest for the evaluation of the systematic uncertainties caused by the use of different elementary operators in the analyses of $\gamma d \to \pi^0 d$ measurements. The calculated differential cross section does not described the TAPS data [4] at backward angles. This discrepancy between theory and experiment maybe resolved by considering the neglected effects from two-body mechanisms in the transition $\mathcal{M}$-matrix. To study the influence of these reaction mechanisms on the $\gamma d \to \pi^0 d$ observables, a more realistic treatment including all possible reaction mechanisms will be reported in a forthcoming paper [63]. An independent evaluation in the framework of effective field theory would also be very interesting. On the experimental side, precise measurements of $\gamma d \to \pi^0 d$ observables can check these predictions and also provide a rigorous test of theoretical models.

Acknowledgments

The authors extend their appreciation to the Deanship of Scientific Research at King Khalid University for funding this work through research groups program under grant number R.G.P.1/1/42. E.M. Darwish would like to thank M.I. Levchuk, V.V. Gauzshtein, and M.N. Nevmerzhitsky for many interesting and helpful discussions.

1. B. Krusche and S. Schadmand, Study of non-strange baryon resonances with meson photoproduction, *Prog. Part. Nucl. Phys.* **51** (2003) 399, https://doi.org/10.1016/S0146-6410(03)90005-6; V. D. Burkert and T.-S. H. Lee, Electromagnetic meson production in the nucleon resonance region, *Int. J. Mod. Phys. E* **13** (2004) 1035, https://doi.org/10.1142/S0218301304002545; K. Helbing, The Gerasimov-Drell-Hearn sum rule, *Prog. Part. Nucl. Phys.* **57** (2006) 405, https://doi.org/10.1016/j.ppnp.2005.09.003; A. Thomas, The Gerasimov-Drell-Hearn sum rule at MAMI, *Eur. Phys. J. A* **28** (2006) 161, https://doi.org/10.1140/epja/i2006-09-017-2; A. M. Sandorfi *et al*., Recent Polarization Experiments and the GDH Sum Rule, *AIP Conf. Proc. 1155* (2009) 73, https://doi.org/10.1063/1.3203304; H. R. Weller *et al*., Research opportunities at the upgraded HIγS facility, *Prog. Part. Nucl. Phys.* **62** (2009) 257, https://doi.org/10.1016/j.ppnp.2008.07.001.

2. B. Krusche, Photoproduction of mesons off nuclei, *Eur. Phys. J. Spec. Topics* **198** (2011) 199, https://doi.org/10.1140/epjst/e2011-01491-2; I. Jaegle (CBELSA/TAPS Collaboration), Quasi-free photoproduction of η-mesons off the deuteron, *Eur. Phys. J. A* **47** (2011) 89, https://doi.org/10.1140/epja/i2011-11089-0; D. K. Hasell *et al*., Spin- Dependent Electron Scattering from Polarized Protons and Deuterons with the BLAST Experiment at MIT-Bates, *Ann. Rev. Nucl. Part. Sci*. **61** (2011) 409, https://doi.org/10.1146/annurev-nucl-100809-131956; B. Strandberg *et al*., Threshold π^- production on the deuteron, *EPJ Web Conf.* **130** (2016) 05019, https://doi.org/10.1051/epjconf/201613005019.

3. B. Strandberg, Ph.D. thesis, University of Glasgow, 2017; S. E. Lukonin *et al.*, Measurement of the tensor analyzing power for the reaction $\gamma d \to pn\pi^0$, *Int. J. Mod. Phys. E* **28** (2019) 1950010, https://doi.org/10.1142/S0218301319500101; B. Strandberg *et al*. (PIONS@Maxlab Collaboration), Near-threshold π^- photoproduction on the deuteron, *Phys. Rev. C* **101** (2020) 035207, https://doi.org/10.1103/PhysRevC.101.035207.

4. U. Siodlaczek, Ph.D. thesis, Tübingen University, 2000; U. Siodlaczek *et al*., Coherent and incoherent π^0 photoproduction from the deuteron, *Eur. Phys. J. A* **10** (2001) 365, https://doi.org/10.1007/s100500170120.

5. D.K. Hasell *et al.*, *Ann. Rev. Nucl. Part. Sci.* **61** (2011) 409.

6. S. A. Zevakov *et al.*, Measuring tensor analyzing power component T_{20} of the coherent photoproduction of a neutral pion on a tensor-polarized deuteron in the VEPP-3 storage ring, *Bull. Russ. Acad. Sci. Phys.* **79** (2015) 864, https://doi.org/10.3103/S1062873815070266; S. A. Zevakov *et al*., Neutral pion photoproduction on tensor-polarized

deuterium on the VEPP-3 storage ring, Bull. *Russ. Acad. Sci. Phys.* **78** (2014) 611, https://doi.org/10.3103/S1062873814070260; D. M. Nikolenko *et al*., Measurement of the tensor analyzing power components in the coherent photoproduction of a π^0 meson on a deuteron, *JETP Lett.* **89** (2009) 432, https://doi.org/10.1134/S0021364009090021; D. M. Nikolenko *et al*., Tensor observables in electro- and photoreactions on the deuteron, *Phys. Part. Nucl.* **48** (2017) 102, https://doi.org/10.1134/S1063779617010154; I. Rachek *et al.*, Measurement of Tensor Analyzing Power T_{20} in Coherent π^0 Photoproduction on Deuteron, *Few Body Syst.* **58** (2017) 29, https://doi.org/10.1007/s00601-016-1191-0; V. V. Gauzshtein *et al*., Measurements of the tensor analyzing power T_{20} of the reaction $\gamma d \rightarrow d\pi^0$, *Int. J. Mod. Phys. E* **29** (2020) 2050011, https://doi.org/10.1142/S0218301320500111; V. V. Gauzshtein *et al*., Measurement of the tensor analyzing power T_{20} for the reaction $\gamma d \rightarrow d\pi^0$, *Eur. Phys. J. A* **56** (2020) 169, https://doi.org/10.1140/epja/s10050-020-00175-z.

7. Y. Ilieva *et al*. (CLAS Collaboration), Coherent Pion Photoproduction on Deuterium, arXiv:nucl-ex/0309017; Y. Ilieva, Evidence for a backward peak in the $\gamma d \rightarrow \pi^0 d$ cross section near the η threshold, *Eur. Phys. J. A* **43** (2010) 261, https://doi.org/10.1140/epja/i2010-10918-x.

8. W. J. Briscoe *et al*., (A2 Collaboration at MAMI), Cross section for $\gamma n \rightarrow \pi^0 n$ measured at the Mainz A2 experiment, *Phys. Rev. C* **100** (2019) 065205, https://doi.org/10.1103/PhysRevC.100.065205; W. J. Briscoe, A. E. Kudryavtsev, I. I. Strakovsky, V. E. Tarasov, and R. L. Workman, Threshold π^- photoproduction on the neutron, *Eur. Phys. J. A* **56** (2020) 218, https://doi.org/10.1140/epja/s10050-020-00221-w; W. J. Briscoe, A. E. Kudryavtsev, I. I. Strakovsky, V. E. Tarasov, and R. L. Workman, On the photoproduction reactions $\gamma d \rightarrow \pi NN$, *Eur. Phys. J. A* **58** (2022) 23, https://doi.org/10.1140/epja/s10050-022-00671-4.

9. D.G. Ireland, E. Pasyuk, and I. Strakovsky, *Prog. Part. Nucl. Phys.* **111** (2020) 103752.

10. V.V.Gauzshtein, E.M. Darwish *et al., Eur. Phys. J. A* **56** (2020) 169.

11. V. V. Gauzshtein *et al*., Measurement of the tensor analyzing power T_{20} for the reaction $\gamma d \rightarrow pn\pi^0$, *Mod. Phys. Lett. A* **36** (2021) 2150199, https://doi.org/10.1142/S0217732321501996.

12. O. Kolesnikov and A. Fix, Three-body calculation of coherent π^0 photoproduction on the deuteron in the Δ region, *J. Phys. G* **48** (2021) 085101, https://doi.org/10.1088/1361-6471/ac010b.

13. T. Ishikawa *et al*. (A2 Collaboration at MAMI), Coherent photoproduction of the neutral-pion and η-meson on the deuteron at incident energies below 1.15 GeV, *Phys. Rev. C* **105** (2022) 045201, https://doi.org/10.1103/PhysRevC.105.045201.

14. F. Cividini *et al*. (A2 Collaboration at MAMI), Measurement of the helicity dependence for single π^0 photoproduction from the deuteron, arXiv:2203.00535.

15. J. H. Koch and R. M. Woloshyn, Near threshold photoproduction of neutral pions from the deuteron, *Phys. Rev. C* **16** (1977) 1968, https://doi.org/10.1103/PhysRevC.16.1968.

16. P. Bosted and J. M. Laget, Electromagnetic properties of the πNN system: (II). The $\gamma D \rightarrow D\pi^0$ reaction, *Nucl. Phys. A* **296** (1978) 413, https://doi.org/10.1016/0375-9474(78)90082-9; J. M. Laget, Electromagnetic properties of the πNN system: (I). The reaction $\gamma D \rightarrow NN\pi$, *Nucl. Phys. A* **296** (1978) 388, https://doi.org/10.1016/0375-9474(78)90081-7; J. M. Laget, Pion photoproduction on few body systems, *Phys. Rep.* **69** (1981) 1, https://doi.org/10.1016/0370-1573(81)90164-2.

17. P. Wilhelm and H. Arenhövel, Dynamical Treatment of the $N\Delta$- Interaction in Photo Reactions on the Deuteron, *Few Body Syst. Suppl.* **7** (1994) 235; P. Wilhelm and H. Arenhövel, Coherent pion photoproduction on the deuteron in the Δ resonance region, *Nucl. Phys. A* **593** (1995) 435, https://doi.org/10.1016/0375-9474(95)00348-5; P. Wilhelm and H. Arenhövel, Rescattering effects in coherent pion photoproduction on the deuteron in the Δ resonance region, *Nucl. Phys. A* **609** (1996) 469, https://doi.org/10.1016/S0375-9474(96)00277-1.

18. H. Garcilazo and E. Moya de Guerra, Pion photoproduction of the deuteron, The reaction $\gamma d \rightarrow \pi^0 d$, **Phys. Rev. C 52** (1995) 49, https://doi.org/10.1103/PhysRevC.52.49; H. Garcilazo and E. Moya de Guerra, Reaction $\gamma d \rightarrow \pi^0 d$ and the small components of the deuteron wave function, *Phys. Rev. C* **49** (1994) R601(R), https://doi.org/10.1103/PhysRevC.49.R601.

19. F. Blaazer, B. L. G. Bakker, and H. J. Boersma, Coherent pion production on the deuteron spin observables, *Nucl. Phys. A* **568** (1994) 681, https://doi.org/10.1016/0375-9474(94)90355-7; F. Blaazer, B. L. G. Bakker, and H. J. Boersma, Rescattering effects in coherent pion production on the deuteron, *Nucl. Phys. A* **590** (1995) 750, https://doi.org/10.1016/0375-9474(95)00218-P; F. Blaazer, Ph.D. thesis, Free University of Amsterdam, 1995.

20. S. S. Kamalov, L. Tiator, and C. Bennhold, Coherent π^0 and η photoproduction on the deuteron, *Phys. Rev. C* **55** (1997) 98, https://doi.org/10.1103/PhysRevC.55.98; S. S. Kamalov, L. Tiator, and C. Bennhold, Polarization observables in pion photoproduction on ^{3}He, *Nucl. Phys. A* **547** (1992) 599, https://doi.org/10.1016/0375-9474(92)90653-2; S. S. Kamalov, L. Tiator, and C. Bennhold, Pion photoproduction on ^{3}He including final-state interaction, *Few Body Syst.* **10** (1991) 143, https://doi.org/10.1007/BF01076291.

21. E. M. Darwish and S. S. Al-Thoyaib, Invariant amplitudes for electromagnetic pion production from the nucleon and its implication for separated structure functions, *Arab. J. Sci. Eng.* **33** (2008) 401; E. M. Darwish and S. S. Al-Thoyaib, Talk presented at the 7th NUPPAC'09 Conference on Nuclear and Particle Physics, November 11-15, 2009, Egypt.

22. E. M. Darwish and M. Y. Hussein, Contribution of coherent pion photoproduction to the Gerasimov-Drell-Hearn sum rule for the deuteron, *Appl. Math. Inf. Sci.* **3** (2009) 321.

23. E. M. Darwish, N. Akopov, and M. El-Zohry, Coherent π^0- photoproduction on the deuteron including polarization observables, *AIP Conf. Proc.* **1370** (2011) 242, https://doi.org/10.1063/1.3638108; E. M. Darwish, N. Akopov, and M. El-Zohry, Coherent π^0-Photoproduction on the Deuteron, Proceeding of the 35th International Conference of High Energy Physics, July 22- 28, Paris, https://doi.org/10.22323/1.120.0185.

24. E. M. Darwish and S. S. Al-Thoyaib, Coherent π^0-photoproduction on the deuteron near the η-production threshold including polarization observables, *Ann. Phys.* **351** (2014) 35, https://doi.org/10.1016/j.aop.2014.08.008; E. M. Darwish and A. Hemmdan, Influence of intermediate ηNN interaction on spin asymmetries for $\gamma d \to \pi^0 d$ reaction near the η-threshold within a three-body approach, *Ann. Phys.* **356** (2015) 128, https://doi.org/10.1016/j.aop.2015.02.035.

25. E. M. Darwish and H. Mansour, Coherent π-Production off Deuteron Near η-Threshold (Lambert Academic Publishing, Saarbrücken, 2015).

26. E. M. Darwish, Influence of the Choice NN Potential Model on $\gamma d \to \pi^0 d$ Observables near η-Threshold, *Chin. Phys. Lett* . **33** (2016) 041301, https://doi.org/10.1088/0256-307X/33/4/041301.

27. E. M. Darwish, H. M. Abou-Elsebaa, and K. S. A. Hassaneen, Tensor Target Spin Asymmetries in Coherent π^0-Photoproduction on the Deuteron Including Intermediate ηNN Interaction Within a Three-Body Approach, *Braz. J. Phys.* **48** (2018) 168, https://doi.org/10.1007/s13538-018-0559-7; E. M. Darwish, E. M. Mahrous, and M. E. Alsehli, Coherent π^0-photoproduction from the deuteron near threshold, *AIP Conf. Proc*. **1976** (2018) 020035, https://doi.org/10.1063/1.5042402.

28. E. M. Darwish, Coherent Photoproduction of π^0-meson from the Deuteron Including Polarization Effects, *Q. Phys. Rev.* **4** (2018) 1729.

29. E. M. Darwish and M. Saleh Yousef, Coherent π^0-Photoproduction on the Deuteron near Threshold and the Role of D-Wave Component of the Deuteron Wave Function, *Moscow Univ. Phys. Bull.* **74** (2019) 595, https://doi.org/10.3103/S0027134919060122.

30. E. M. Darwish, H. M. Abou-Elsebaa, Kh. S. Alsadi, and M. Saleh Yousef, The Spin Response of the $\gamma d \to \pi^0 d$ Reaction Near Threshold and Its Implication to the GDH Sum Rule and the Double Polarization E- Asymmetry, *Moscow Univ. Phys. Bull*. **75** (2020) 198, https://doi.org/10.3103/S002713492003008X.

31. H. M. Al-Ghamdi, E. S. Almogai, E. M. Darwish, and S. Abdel-Khalek, Beam-target double spin asymmetries in the reaction $\gamma d \to \pi^0 d$ near threshold and the role of D-wave component of the deuteron wave function, *Braz. J. Phys.* **50** (2020) 615, https://doi.org/10.1007/s13538-020-00771-w.

32. H. Al-Ghamdi, E. S. Almogait, E. M. Darwish, and S. Abdel-Khalek, Tensor analyzing power component T_{20} of the $\gamma \vec{d} \to \pi^0 d$ process in the photon energy range from 200 to 400 MeV, *Res. Phys.* **18** (2020) 103238, https://doi.org/10.1016/j.rinp.2020.103238.

33. E. M. Darwish and H. M. Al-Ghamdi, Sensitivity of Polarization Observables in $\gamma d \to \pi^0 d$ Reaction Near Threshold to the Choice of Elementary $\gamma N \to \pi N$ Amplitude and Deuteron Wave Function, *Moscow Univ. Phys. Bull.* **76** (2021) 136, https://doi.org/10.3103/S0027134921030036.

34. E. M. Darwish, C. Fernández-Ramírez, E. Moya de Guerra, and J. M. Udías, Helicity dependence and contribution to the Gerasimov-Drell-Hearn sum rule of the $\vec{\gamma}\vec{d} \to \pi NN$ reaction channels in the energy region from threshold up to the $\Delta(1232)$ resonance, *Phys. Rev. C* **76** (2007) 044005, https://doi.org/10.1103/PhysRevC.76.044005.

35. M. I. Levchuk, Helicity-dependent reaction $\vec{\gamma}\vec{d} \to \pi NN$ and its contribution to the Gerasimov- Drell-Hearn sum rule for the deuteron, *Phys. Rev. C* **82** (2010) 044002, https://doi.org/10.1103/PhysRevC.82.044002.

36. E. M. Darwish and S. S. Al-Thoyaib, Incoherent pion photoproduction on the deuteron including polarization effects, *Ann. Phys.* **326** (2011) 604, https://doi.org/10.1016/j.aop.2010.09.014.

37. E. M. Darwish, M. M. Almarashi, E. M. Mahrous, M. A. Hassanain, and M. Saleh Yousef, Near-threshold incoherent pion photoproduction on the deuteron with final-state interaction effects, *Ann. Phys.* **411** (2019) 167990, https://doi.org/10.1016/j.aop.2019.167990.

38. E. M. Darwish, M. M. Almarashi, and M. Saleh Yousef, Beam-targeet double spin asymmetries in the reaction $\vec{\gamma}\vec{d} \to \pi NN$ near threshold with final-state rescattering effects, *Ann. Phys.* **420** (2020) 168254, https://doi.org/10.1016/j.aop.2020.168254.

39. E. M. Darwish, M. I. Levchuk, M. N. Nevmerzhitsky, M. M. Almarashi, and M. Saleh Yousef, Influence of rescattering effects on the helicity dependence of $\vec{\gamma}\vec{d} \to \pi NN$ near threshold and its implication to the E-asymmetry and the GDH sum rule, *Chin. J. Phys.* **71** (2021) 319, https://doi.org/10.1016/j.cjph.2020.07.015.

40. R. A. Arndt, W. J. Briscoe, I. I. Strakovsky, and R. L. Workman, Analysis of pion photoproduction data, *Phys. Rev. C* **66** (2002) 055213, https://doi.org/10.1103/PhysRevC.66.055213.

41. D. Drechsel, O. Hanstein, S. S. Kamalov, and L. Tiator, A unitary isobar model for pion photo- and electroproduction on the proton up to 1 GeV, *Nucl. Phys. A* **645** (1999) 145, https://doi.org/10.1016/S0375-9474(98)00572-7.

42. A. V. Anisovich *et al.*, Photoproduction of baryons decaying into $N\pi$ and $N\eta$, *Eur. Phys. J. A* **25** (2005) 427, https://doi.org/10.1140/epja/i2005-10120-5; A. V. Anisovich, E. Klempt, A. V. Sarantsev, and U. Thoma, Partialwave decomposition of pion and photoproduction amplitudes, *Eur. Phys. J. A* **24** (2005) 111, https://doi.org/10.1140/epja/i2004-10125-6; A. V. Anisovich *et al.*, Properties of baryon resonances from a multichannel partial wave analysis, *Eur. Phys. J. A* **48** (2012) 15, https://doi.org/10.1140/epja/i2012-12015-8.

43. T. Sato and T.-S. H. Lee, Meson-exchange model for πN scattering and $\gamma N \to \pi N$ reaction, *Phys. Rev. C* **54** (1996) 2660, https://doi.org/10.1103/PhysRevC.54.2660; T. Sato and T.-S. H. Lee, Dynamical study of the

Δ excitation in $N(e,e'\pi)$ reactions, *Phys. Rev. C* **63** (2001) 055201, https://doi.org/10.1103/PhysRevC.63.055201; H. Kamano, S. X. Nakamura, T.-S. H. Lee, and T. Sato, Nucleon resonances within a dynamical coupled-channels model of πN and γN reactions, *Phys. Rev. C* **88** (2013) 035209, https://doi.org/10.1103/PhysRevC.88.035209; H. Kamano, T.-S. H. Lee, S. X. Nakamura, and T. Sato, The ANL-Osaka Partial-Wave Amplitudes of πN and γN reactions, arXiv:1909.11935.

44. T. Feuster and U. Mosel, Unitary model for meson-nucleon scattering, *Phys. Rev. C* **58** (1998) 457, https://doi.org/10.1103/PhysRevC.58.457; V. Shklyar, H. Lenske, and U. Mosel, Analysis of baryon resonances in the coupled-channel Giessen model, Proceedings of the 11th Workshop on The Physics of Excited Nucleons, September 5-8, Bonn, https://doi.org/10.1007/978-3-540-85144-8_16; V. Shklyar, H. Lenske, and U. Mosel, η photoproduction in the resonance energy region, *Phys. Lett. B* **650** (2007) 172, https://doi.org/10.1016/j.physletb.2007.05.005; V. Shklyar, H. Lenske, and U. Mosel, Giessen coupled-channel model for pion- and photon-induced reactions, **AIP Conf. Proc. 1432** (2012) 349, https://doi.org/10.1063/1.3701246.

45. C. Fernández-Ramírez, E. Moya de Guerra, and J. M. Udías, Crossing symmetry and phenomenological widths in effective Lagrangian models of the pion photoproduction process, *Phys. Lett. B* **660** (2008) 188, https://doi.org/10.1016/j.physletb.2007.11.099; C. FernÃ¡ndez-RamÃrez, Ph.D. tesis, Universidad Complutense de Madrid, 2006.

46. D. Drechsel, S. S. Kamalov, and L. Tiator, Unitary isobar model- MAID2007, *Eur. Phys. J. A* **34** (2007) 69, https://doi.org/10.1140/epja/i2007-10490-6.

47. S. S. Kamalov and S. Nan Yang, Pion Cloud and the Q^2 Dependence of $\gamma^* N \leftrightarrow \Delta$ Transition Form Factors, *Phys. Rev. Lett.* **83** (1999) 4494, https://doi.org/10.1103/PhysRevLett.83.4494; S. S. Kamalov, S. Nan Yang, D. Drechsel, O. Hanstein, and L. Tiator, $\gamma^* N \rightarrow \Delta$ transition form factors: A new analysis of data on $p(e,e'p)\pi^0$ at $Q^2 = 2.8$ and 4.0 (GeV/c)^2, *Phys. Rev. C* **64** (2001) 032201(R), https://doi.org/10.1103/PhysRevC.64.032201.

48. M. Hilt, S. Scherer, and L. Tiator, Threshold π^0 photoproduction in relativistic chiral perturbation theory, *Phys. Rev. C* **87** (2013) 045204, https://doi.org/10.1103/PhysRevC.87.045204; M. Hilt, B. C. Lehnhart, S. Scherer, and L. Tiator, Pion photo- and electroproduction in relativistic baryon chiral perturbation theory and the chiral MAID interface, *Phys. Rev. C* **88** (2013) 055027, https://doi.org/10.1103/PhysRevC.88.055207.

49. S. B. Gerasimov, A sum rule for magnetic moments and the damping of the nucleon magnetic moment in nuclei, *Yad. Fiz.* **2** (1965) 598 [*Sov. J. Nucl. Phys.* **2** (1966) 430]; S. D. Drell and A. C. Hearn, Exact Sum Rule for Nucleon Magnetic Moments, *Phys. Rev. Lett.* **16** (1966) 908, https://doi.org/10.1103/PhysRevLett.16.908.

50. H. Arenhövel, General formulae for polarization observables in two-body break-up of deuteron photodisintegration, *Few Body Syst.* **4** (1988) 55, https://doi.org/10.1007/BF01076329.

51. J. D. Bjorken and S. D. Drell, Relativistic Quantum Mechanics (McGraw- Hill, New York, 1964).

52. H. Arenhövel, Invariant Amplitudes for Coherent Electromagnetic Pseudoscalar Production from a Spin-One Target, II: Crossing, Multipoles, and Observables, *Few Body Syst.* **27** (1999) 141, https://doi.org/10.1007/s006010050127.

53. A. R. Edmonds, Angular Momentum in Quantum Mechanics (Princeton University Press, New Jersey, 1957).

54. H. Arenhövel, Spin degrees and polarization observables in electromagnetic reactions, *Int. J. Mod. Phys. E* **18** (2009) 1226, https://doi.org/10.1142/S0218301309013476.

55. R. Machleidt, K. Holinde, and Ch. Elster, The Bonn meson-exchange model for the nucleon-nucleon interaction, *Phys. Rep.* **149** (1987) 1, https://doi.org/10.1016/S0370-1573(87)80002-9.

56. R. Machleidt, High-precision, charge-dependent Bonn nucleon-nucleon potential, *Phys. Rev. C* **63** (2001) 024001, https://doi.org/10.1103/PhysRevC.63.024001.

57. M. Lacombe *et al*., Parametrization of the deuteron wave function of the Paris N-N potential, *Phys. Lett. B* **101** (1981) 139, https://doi.org/10.1016/0370-2693(81)90659-6.

58. B. D. Day, Nuclear Saturation from Two-Nucleon Potentials, *Phys. Rev. Lett.* **47** (1981) 226, https://doi.org/10.1103/PhysRevLett.47.226.

59. M. Hjorth-Jensen, T. T. S. Kuo, and E. Osnes, Realistic effective interactions for nuclear systems, *Phys. Rep.* **261** (1995) 125, https://doi.org/10.1016/0370-1573(95)00012-6.

60. E. M. Darwish, H. M. Abou-Elsebaa, E. M. Mahrous, and S. S. Al-Thoyaib, Sensitivity of tensor and vector analyzing powers in elastic $e-d$ scattering to modern local and non-local NN potentials, *Ind. J. Phys.* **94** (2020) 1025, https://doi.org/10.1007/s12648-019-01537-0.

61. M. Benmerrouche and E. Tomusiak, $\gamma D \rightarrow \pi^0 D$ reaction in the threshold region, *Phys. Rev. C* **58** (1998) 1777, https://doi.org/10.1103/PhysRevC.58.1777.

62. J. A. Gómez Tejedor, S. S. Kamalov, and E. Oset, Meson Exchange currents in the ^{3}He$(\gamma,\pi^+)^3$H reaction, *Phys. Rev. C* **54** (1996) 3160, https://doi.org/10.1103/PhysRevC.54.3160.

63. M.I. Levchuk, V.V.Gauzshtein, E.M. Darwish, M.N. Nevmerzhitsky, (in preparation).